THE UNIVERSITY OF CHICAGO
PRITZKER SCHOOL OF MOLECULAR ENGINEERING

Argonne NATIONAL LABORATORY

Q-NEXT NEXT GENERATION QUANTUM SCIENCE AND ENGINEERING

# Development of erbium-doped oxide thin films for quantum communication platforms

***Thesis Defense – Gregory Grant – Guha Group – September 13, 2024***

*To the committee of:*
*Prof. Supratik Guha, Prof. David Awschalom, Dr. F. Joseph Heremans*

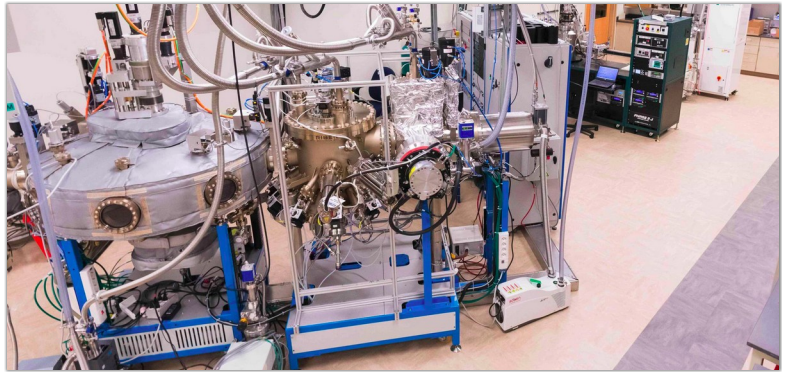

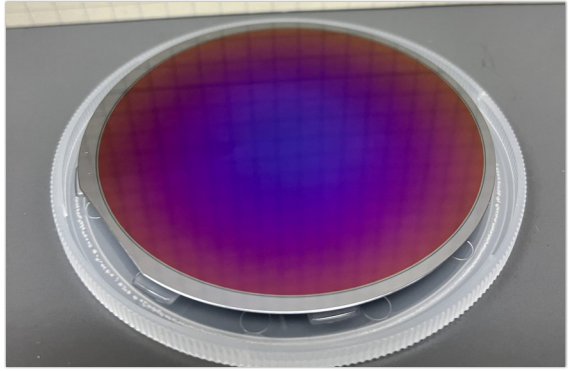

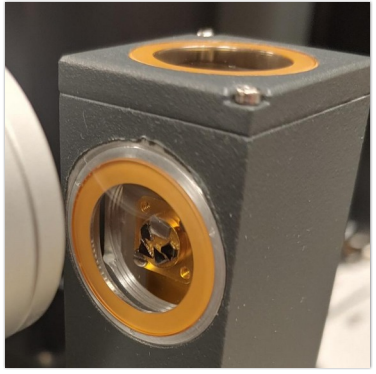

# Thesis Defense Outline



1. Discussion on selecting a quantum communication-relevant defect
2. Review of erbium energy structure and aspects relevant to our work
3. Developing $CeO_2$ as a host for Er
4. Expanding $CeO_2$ to other substrates for alternative integrations
5. Considering other host materials for Er via computational survey
6. Conclusions and final remarks

# Thesis Defense Outline



**1. Discussion on selecting a quantum communication-relevant defect**

2. Review of erbium energy structure and aspects relevant to our work

3. Developing $CeO_2$ as a host for Er

4. Expanding $CeO_2$ to other substrates for alternative integrations

5. Considering other host materials for Er via computational survey

6. Conclusions and final remarks

# The goal of quantum communication

THE UNIVERSITY OF CHICAGO
PRITZKER SCHOOL OF MOLECULAR ENGINEERING
Argonne NATIONAL LABORATORY
Q-NEXT NEXT GENERATION QUANTUM SCIENCE AND ENGINEERING


[1]

$$|\psi\rangle = \alpha\,|0\rangle + \beta\,|1\rangle$$

**Goal:** We want to distribute quantum states across long channels, e.g., between cities.

$$|\psi\rangle \not\rightarrow |\psi\rangle\,|\psi\rangle\,|\psi\rangle$$

**Problem:** No-cloning forbids state duplication, so we cannot amplify weak quantum signals

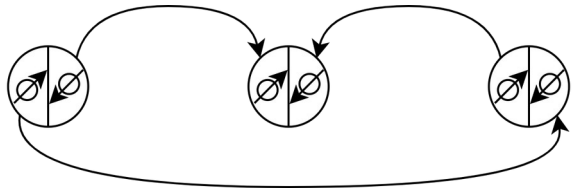

**Solution:** Quantum repeaters reduce overall loss, but need synchronization between nodes using quantum memory

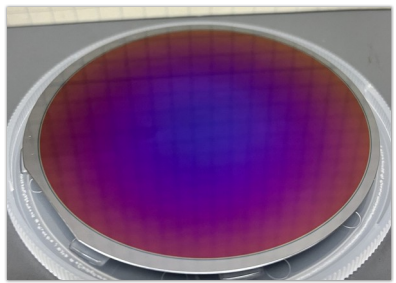

**Implementation:** Solid state quantum memory leverages well established fabrication techniques

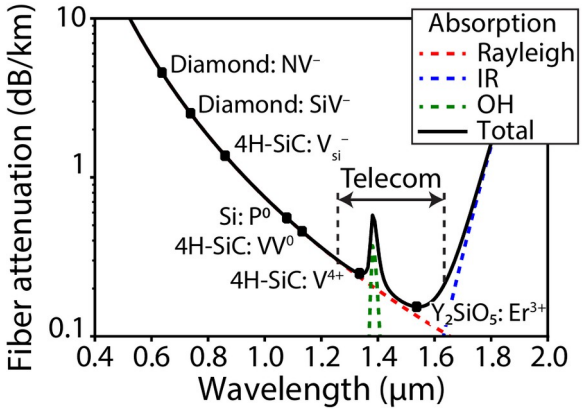


Attenuation through a fiber optic at varied wavelengths, with the **minimum at 1.5 μm** [2]

**Requirements:** A memory qubit must have an energy structure: with a telecom interface and long-coherence storage; preferably in a Si-compatible host

[1]: https://news.uchicago.edu/story/chicago-quantum-network-argonne-pritzker-molecular-engineering-toshiba
[2]: Wolfowicz et al, *Nat. Rev. Mat.*, 6.10 (2021)

# Designating a quantum memory qubit



**Recall Requirements:** A memory qubit must have an energy structure with the following:
- A telecom-wavelength transition as an interface
- A long-coherence-time transition as a storage mechanism

**Interface mechanism**: Read and write from the storage state; interacts with the environment
- Fast lifetime $T_1$, telecom wavelengths

**Storage mechanism**: Keep a state with high fidelity for a long time; isolated from environment
- Long coherence $T_2$, controllable with driving field

Let's pick a defect to facilitate this.

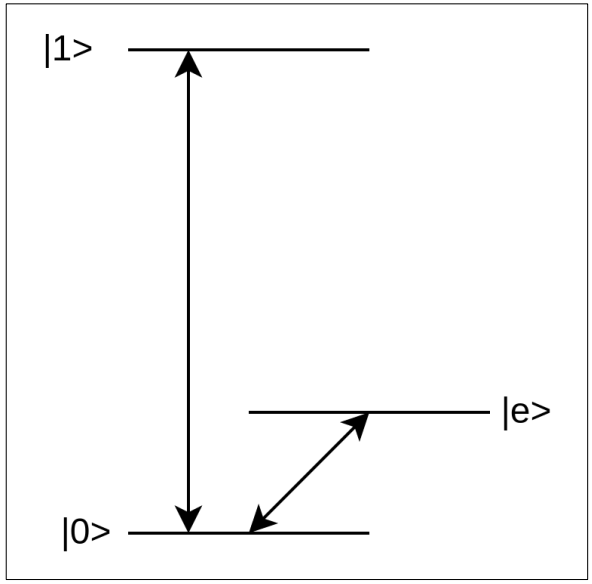


Archetypal 3-level system

# Selecting erbium for quantum memory

THE UNIVERSITY OF CHICAGO
PRITZKER SCHOOL OF MOLECULAR ENGINEERING
Argonne NATIONAL LABORATORY
Q-NEXT NEXT GENERATION QUANTUM SCIENCE AND ENGINEERING

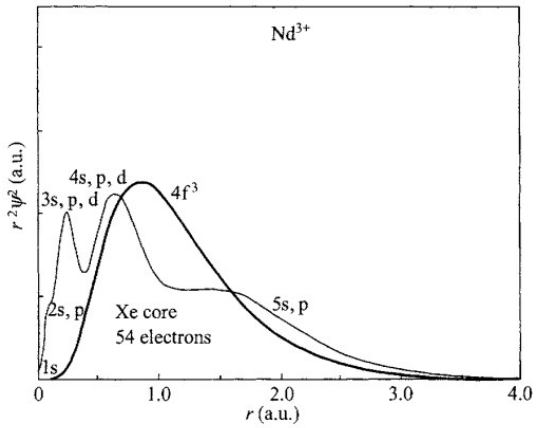


Radial wavefunction of $Nd^{3+}$ compared to Xe core charge distribution – note **shielded** 4f extent [1]

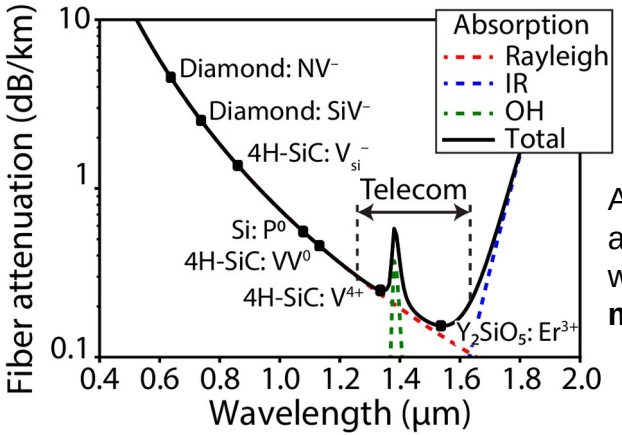


Attenuation through a fiber optic at varied wavelengths, with the **minimum at 1.5 μm** [2]

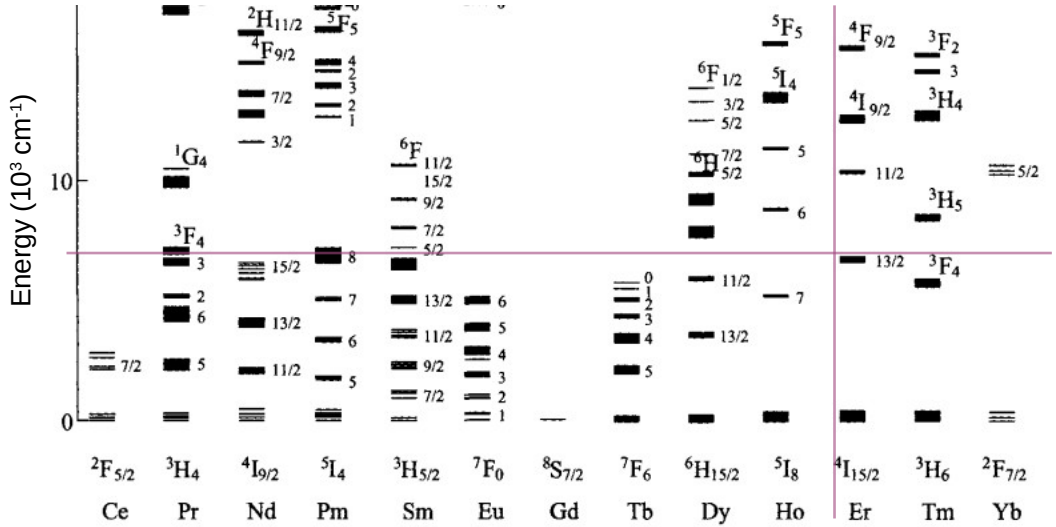


Energy structure of $R^{3+}$:$LaF_2$ (N.B.: 1538 nm = 6500 $cm^{-1}$) [1]

**$Er^{3+}$** is demonstrated to have **long spin and optical quantum coherence times**, e.g. 4ms $T_{2,opt}$ in Er:YSO at 2 K [1] and 23ms $T_{2,spin}$ in $CaWO_4$ at 10 mK [3]

The only downside is that Er is dim.

[1]: Liu and Jacquier, *Spect. Prop. of Rare Earths*, 2005
[2]: Wolfowicz et al, *Nat. Rev. Mat.*, 6.10 (2021)
[3]: Dantec et al, *Sci. Adv.*, 7.51 (2021)

# Thesis Defense Outline



1. Discussion on selecting a quantum communication-relevant defect
2. **Review of erbium energy structure and aspects relevant to our work**
3. Developing $CeO_2$ as a host for Er
4. Expanding $CeO_2$ to other substrates for alternative integrations
5. Considering other host materials for Er via computational survey
6. Conclusions and final remarks

# Is the erbium energy structure viable?

THE UNIVERSITY OF CHICAGO
PRITZKER SCHOOL OF MOLECULAR ENGINEERING
Argonne NATIONAL LABORATORY
Q-NEXT NEXT GENERATION QUANTUM SCIENCE AND ENGINEERING

We wish to identify an archetypal 3-level system within the energy structure of erbium, here via close examination of its Hamiltonian. [1,2]

Starting point: An N-electron atom

$$H = -\frac{\hbar^2}{2m}\sum_{i=1}^{N}\nabla_i^2 - \sum_{i=1}^{N}\frac{Ze^2}{r_i} + \sum_{i<j}^{N}\frac{e^2}{r_{ij}}$$

Refinement: “Central Field” approximation

$$H = H_{\mathrm{CF}} + H_c, \quad H_{\mathrm{CF}} = \sum_{i=1}^{N}\left(-\frac{\hbar^2}{2m}\nabla_i^2 + U(r_i)\right)$$

The central field Hamiltonian lets us use hydrogenic wavefunctions as our basis.

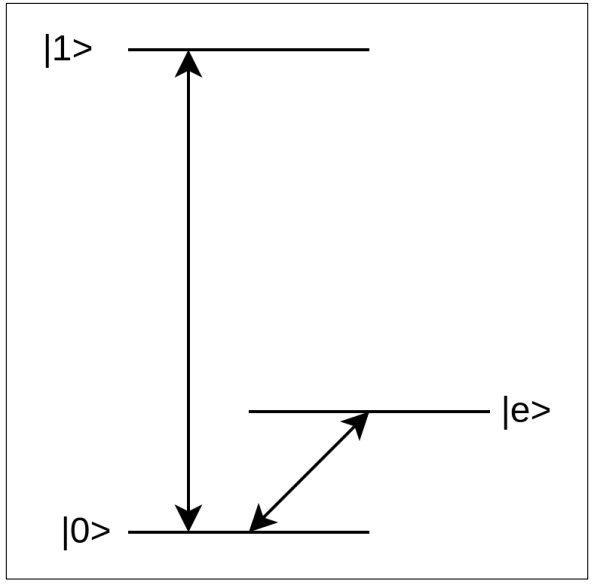


Archetypal 3-level system



[1]: Judd, *Operator Techniques in Atomic Spectroscopy*, 1963
[2]: Wybourne, *Spectroscopic Properties of Rare Earths*, 1965

# Working beyond the central field



$$H = H_{\mathrm{CF}} + H_c, \quad H_{\mathrm{CF}} = \sum_{i=1}^{N} \Big( -\frac{\hbar^2}{2m}\nabla_i^2 + U(r_i) \Big)$$

$$H_c = \sum_{i=1}^{N} \Big( -\frac{Ze^2}{r_i} - U(r_i) \Big) + \sum_{i>j=1}^{N} \frac{e^2}{r_{ij}}$$

Looking at the terms external to the central field, we find $H_1$:

$$H_1 = \sum_{i>j=1}^{N} \frac{e^2}{r_{ij}}$$ (the inter-electron Coulomb potential)

Then we start adding other perturbations, such as spin-orbit:

$$H_2 = \sum_{i=1}^{N} \xi(r_i)\boldsymbol{s}_i \cdot \boldsymbol{l}_i, \qquad \xi(r) = \frac{\hbar^2}{2m^2c^2r}\frac{\mathrm{d}U}{\mathrm{d}r}$$

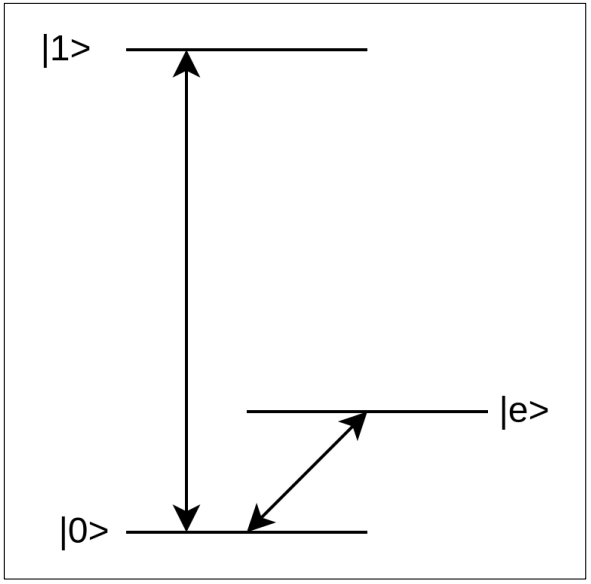


Archetypal 3-level system



[1]: Judd, *Operator Techniques in Atomic Spectroscopy*, 1963
[2]: Wybourne, *Spectroscopic Properties of Rare Earths*, 1965

# Splitting Er states into terms

THE UNIVERSITY OF CHICAGO
PRITZKER SCHOOL OF MOLECULAR ENGINEERING
Argonne NATIONAL LABORATORY
Q-NEXT NEXT GENERATION QUANTUM SCIENCE AND ENGINEERING

Inter-electron Coulomb potential

$$H_1 = \sum_{i>j=1}^{N} \frac{e^2}{r_{ij}}$$

Spin-orbit coupling potential:

$$H_2 = \sum_{i=1}^{N} \xi(r_i)\boldsymbol{s}_i \cdot \boldsymbol{l}_i, \qquad \xi(r) = \frac{\hbar^2}{2m^2c^2r}\frac{\mathrm{d}U}{\mathrm{d}r}$$

This gives us a framework to discuss electron configurations (using LS coupling here):

$$\boldsymbol{L} = \sum_i \boldsymbol{l}_i \qquad \boldsymbol{S} = \sum_i \boldsymbol{s}_i \longrightarrow {}^{2S+1}L_J$$

$$\boldsymbol{J} = \boldsymbol{S} + \boldsymbol{L}$$

Er energy levels upon "turning on" $H_1$ and $H_2$

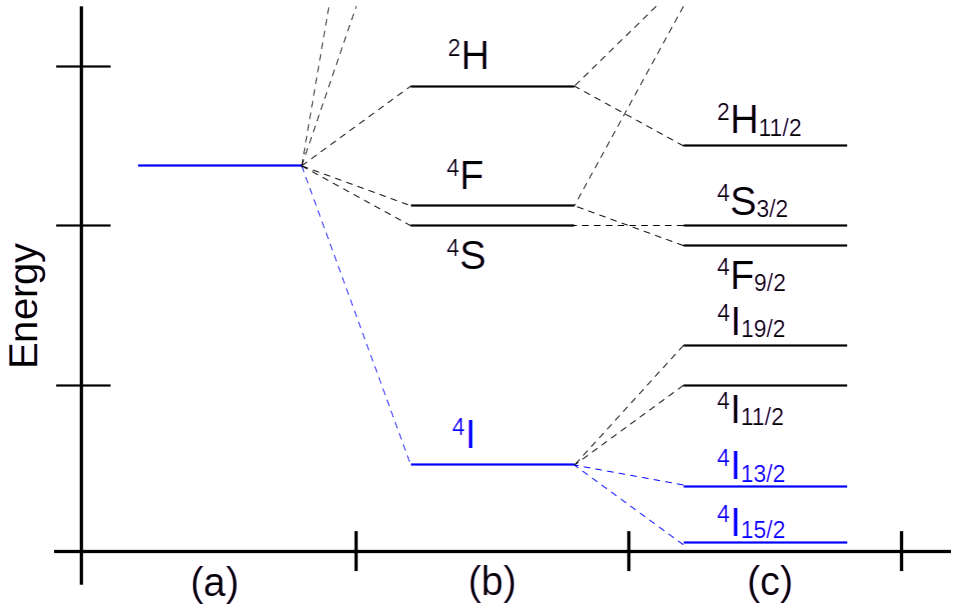


*L* is written in spectroscopic notation, so 1=S, 1=P, 2=D, …, 6=I, ...

[1]: Judd, *Operator Techniques in Atomic Spectroscopy*, 1963
[2]: Wybourne, *Spectroscopic Properties of Rare Earths*, 1965

# Splitting Er terms into crystal field levels

THE UNIVERSITY OF CHICAGO
PRITZKER SCHOOL OF MOLECULAR ENGINEERING
Argonne NATIONAL LABORATORY
Q-NEXT NEXT GENERATION QUANTUM SCIENCE AND ENGINEERING

We can apply additional perturbations based on the environment around the Er.

The crystal field (electric potential) perturbation:

$$H_3 = -e\sum_i V_e(r_i, \theta_i, \phi_i)$$

External magnetic field and hyperfine splitting:

$$H_{4-5} = \beta \boldsymbol{B} \cdot \boldsymbol{g} \cdot \boldsymbol{S} + A\boldsymbol{S} \cdot \boldsymbol{I}$$

$H_3$ in particular splits Er into the “crystal field levels” which are each doubly degenerate.

Er energy levels upon “turning on” $H_3$ and $H_{4\text{-}5}$

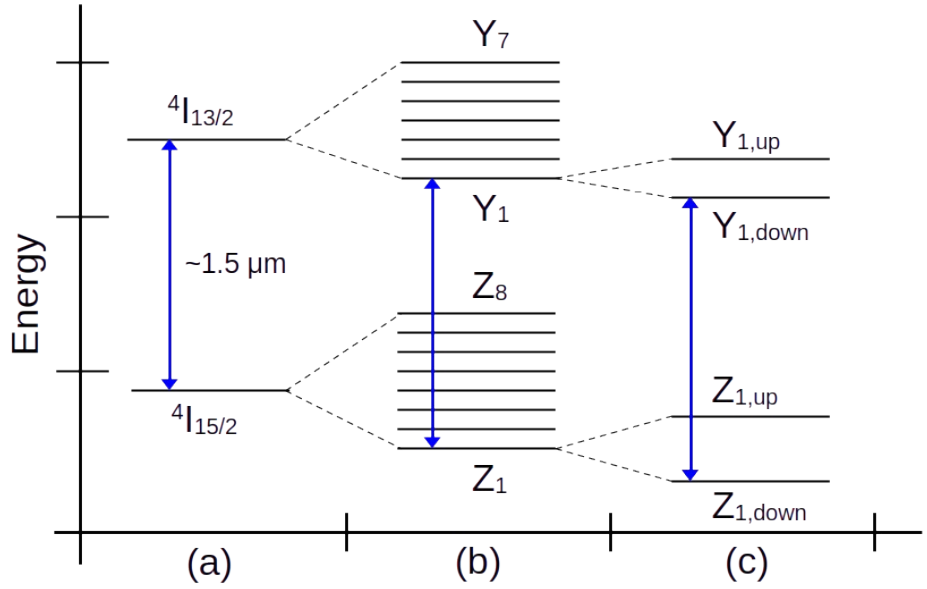




[1]: Judd, *Operator Techniques in Atomic Spectroscopy*, 1963
[2]: Wybourne, *Spectroscopic Properties of Rare Earths*, 1965

# Comparing Er levels with our archetype

THE UNIVERSITY OF CHICAGO
PRITZKER SCHOOL OF MOLECULAR ENGINEERING
Argonne NATIONAL LABORATORY
Q-NEXT NEXT GENERATION QUANTUM SCIENCE AND ENGINEERING

$$H_1 = \sum_{i>j=1}^{N} \frac{e^2}{r_{ij}}$$

$$H_2 = \sum_{i=1}^{N} \xi(r_i)\boldsymbol{s}_i \cdot \boldsymbol{l}_i,$$

$$H_3 = -e \sum_i V_e(r_i, \theta_i, \phi_i)$$

$$H_{4-5} = \beta \boldsymbol{B} \cdot \boldsymbol{g} \cdot \boldsymbol{S}$$

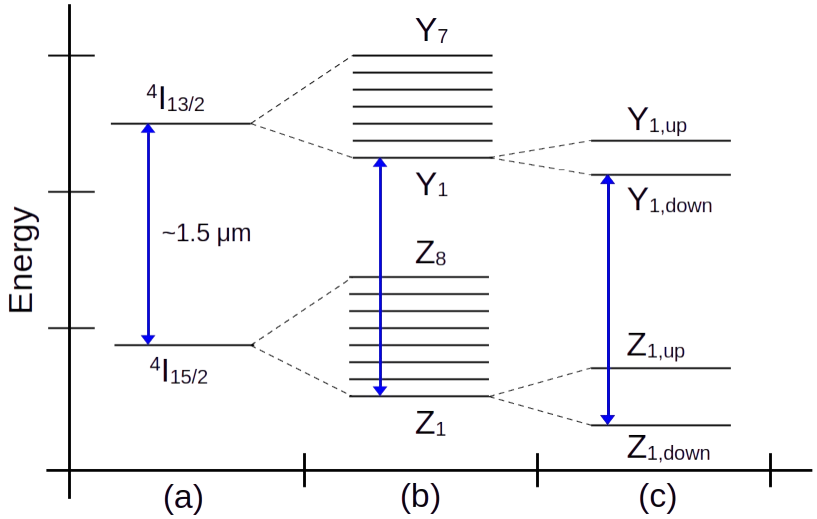


Working through the Er energy structure, we've found an archetypal qubit level structure in **the Zeeman-split $Z_1$-$Y_1$ transition**!

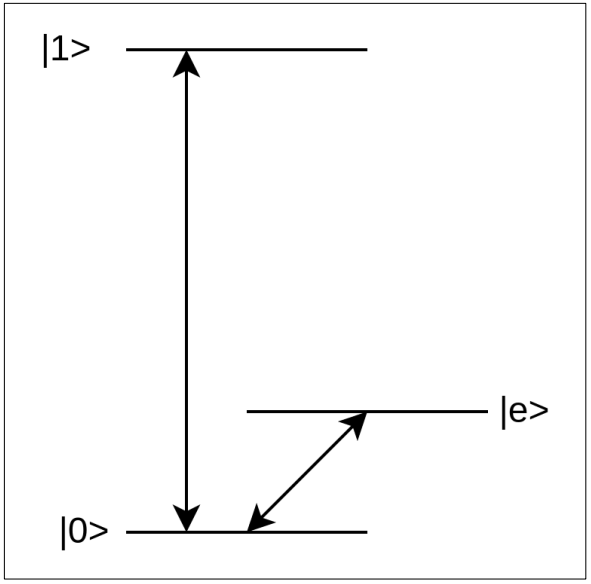


Archetypal 3-level system



[1]: Judd, *Operator Techniques in Atomic Spectroscopy*, 1963
[2]: Wybourne, *Spectroscopic Properties of Rare Earths*, 1965

# Thesis Defense Outline



1. Discussion on selecting a quantum communication-relevant defect
2. Review of erbium energy structure and aspects relevant to our work
3. **Developing $CeO_2$ as a host for Er**
4. Expanding $CeO_2$ to other substrates for alternative integrations
5. Considering other host materials for Er via computational survey
6. Conclusions and final remarks

# Why use $CeO_2$ to host erbium?

THE UNIVERSITY OF CHICAGO
PRITZKER SCHOOL OF MOLECULAR ENGINEERING
Argonne NATIONAL LABORATORY
Q-NEXT NEXT GENERATION QUANTUM SCIENCE AND ENGINEERING

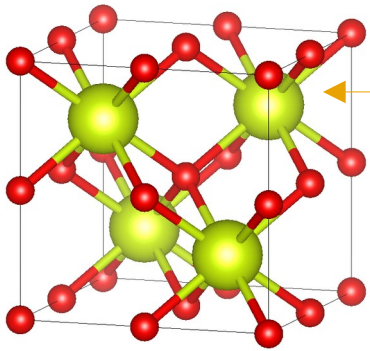

O: 99.8% nuclear spin 0

Ce: 100% nuclear spin 0

Fluorite structure
$O_h$ symmetry Ce site
a = 5.41 Å (ICDD)

$CeO_2$ predicted to be an optimal defect host:
- **Predicted defect spin $T_2$ of 47 ms due to low nuclear spin environment [1]**
- Wide band gap (~3 eV > 0.8 eV)

Also a good candidate for growth study:
- Straightforward to grow in MBE
- Grows epitaxially on silicon (<0.5% mismatch)
- Lessons learned can transfer to other oxides

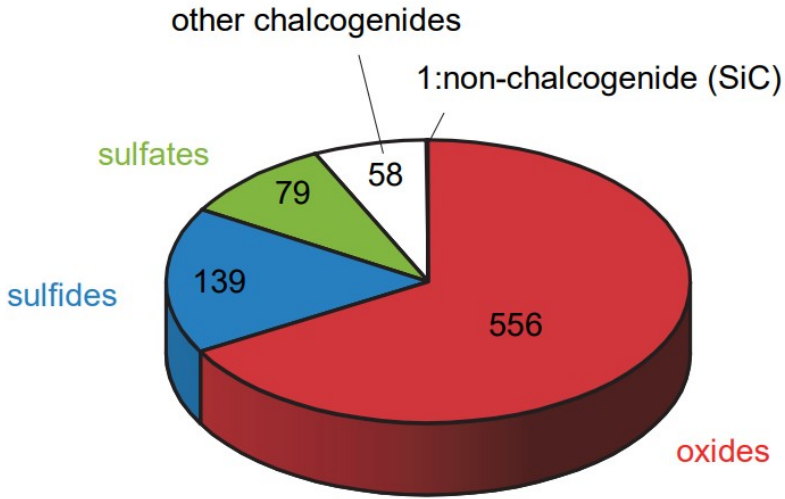


Inventory of stable compounds with theoretical $T_{2,Hahn}$ > 1 ms and bandgap above 1 eV [1]

[1]: Kanai et al, *PNAS*, 199(15), e2121808119 (2022)

# Growing Er:$CeO_2$ via MBE

THE UNIVERSITY OF CHICAGO
PRITZKER SCHOOL OF MOLECULAR ENGINEERING
Argonne NATIONAL LABORATORY
Q-NEXT NEXT GENERATION QUANTUM SCIENCE AND ENGINEERING

Molecular beam epitaxy (MBE) recipe:
1. Start with base growth chamber pressure of $10^{-9}$ torr
2. Prepare Si(111) substrate, RCA cleaned with HF step last
3. Flash substrate pre-growth for 7x7 surface reconstruction
4. Evaporate high-purity cerium and erbium metal; flow oxygen

Growth parameters:
- **Growth rate of up to 50-300 nm/hr** upon a 670 $^{o}$C substrate
- Erbium doping controllable via cell temp, **from sub-ppm to 100s ppm**

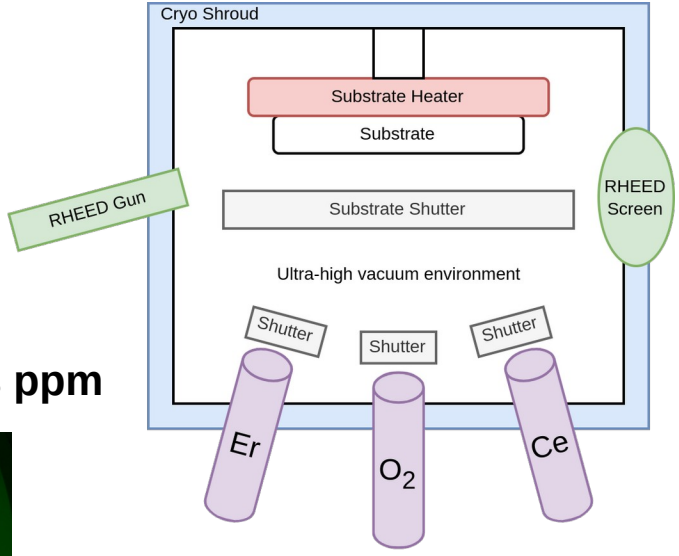


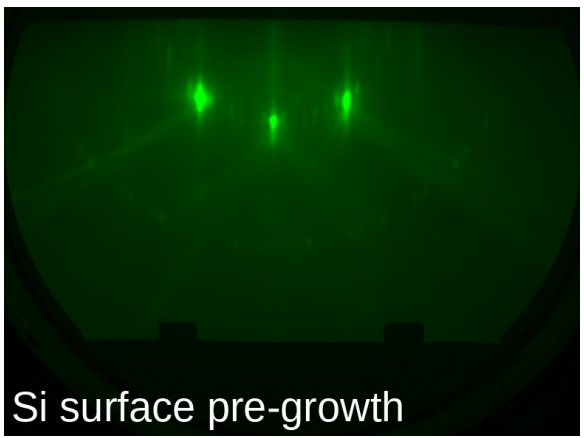


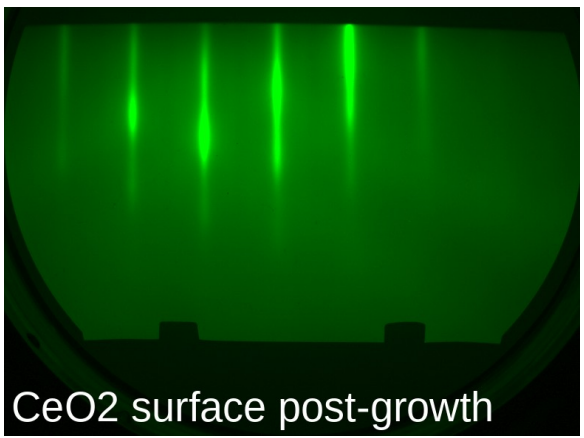


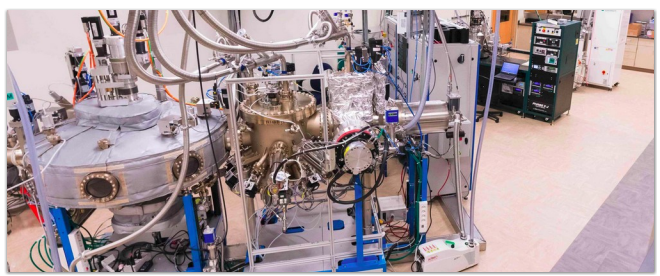



Grant et al, *APL Materials*, 12, 021121 (2024)

# Establishing a growth window for $CeO_2$

THE UNIVERSITY OF CHICAGO
PRITZKER SCHOOL OF MOLECULAR ENGINEERING
Argonne NATIONAL LABORATORY
Q-NEXT NEXT GENERATION QUANTUM SCIENCE AND ENGINEERING

We tune the ratio of Ce and $O_2$ fluxes for single crystalline growth.

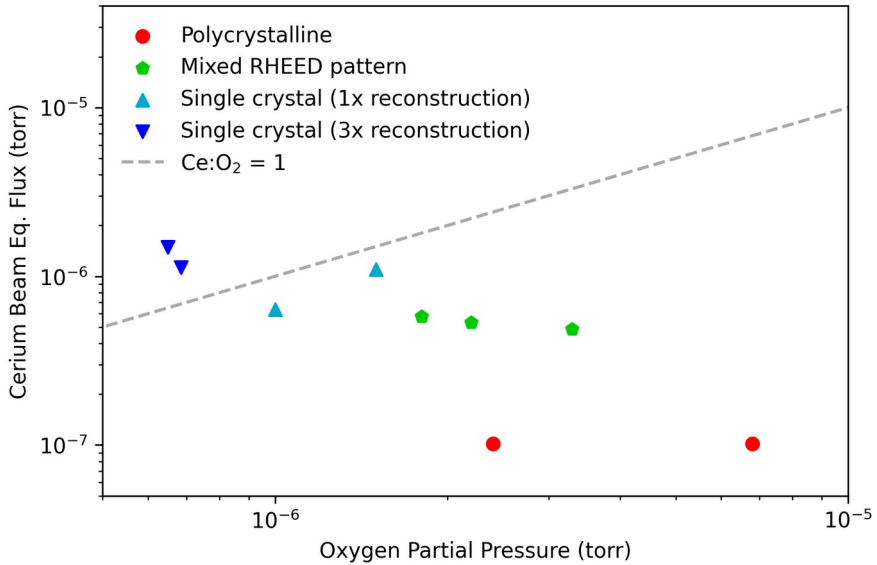


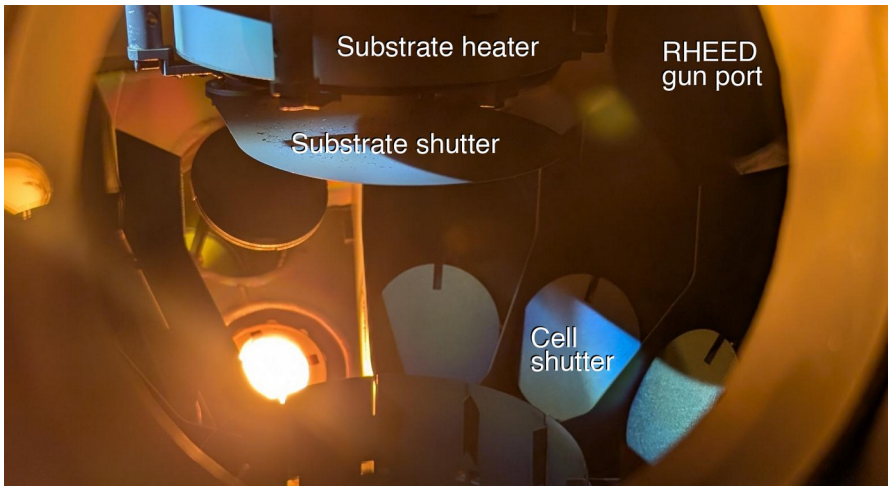


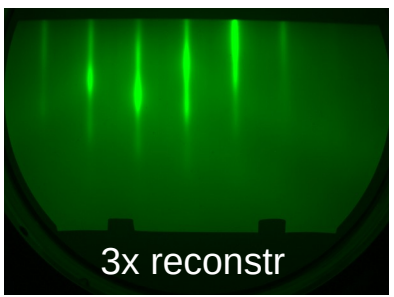


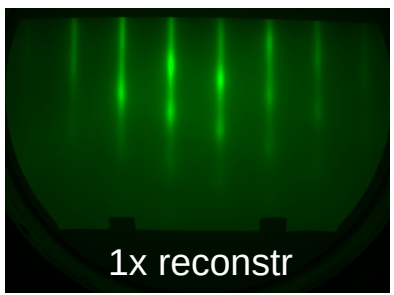


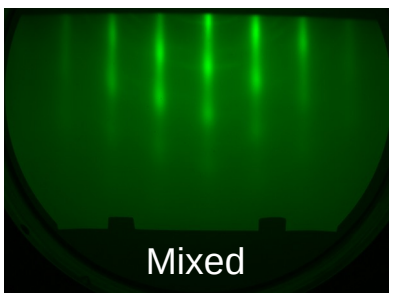


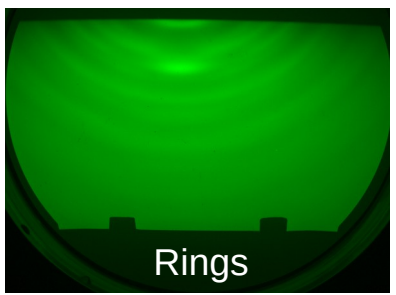




Grant et al, *APL Materials*, 12, 021121 (2024)

# Control of Er doping level during growth

THE UNIVERSITY OF CHICAGO
PRITZKER SCHOOL OF MOLECULAR ENGINEERING
Argonne NATIONAL LABORATORY
Q-NEXT NEXT GENERATION QUANTUM SCIENCE AND ENGINEERING

We can adjust the amount of Er in the $CeO_2$ film based on the Er cell temperature and the $CeO_2$ growth rate.

| $CeO_2$ Growth Rate (nm/hr) | $T_{Er} = 800$ °C | $T_{Er} = 900$ °C | $T_{Er} = 1000$ °C |
|---|---|---|---|
| 25 | 2.5 ppm | 45 ppm | 503 ppm |
| 50 | 1.3 ppm | 22 ppm | 251 ppm |
| 100 | 0.6 ppm | 11 ppm | 126 ppm |
| 200 | 0.3 ppm | 6 ppm | 63 ppm |

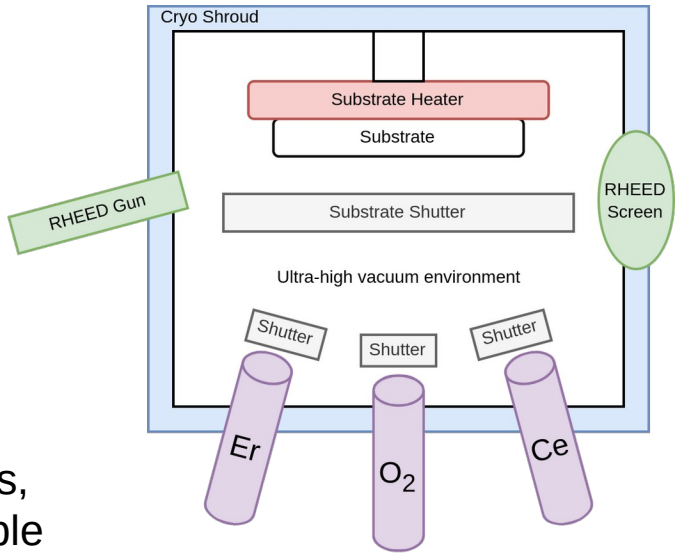


Er concentration impacts things like oxygen vacancy concentrations, and alters average Er-Er distances – leading to changes in ensemble interactions.

| *Er Doping Level (ppm)* | 1 | 10 | 100 (0.01%) | 1,000 (0.1%) | 10,000 (1%) |
|---|---|---|---|---|---|
| *Mean Distance to Nearest Er (Å)* | 190 | 90 | 40 | 20 | 9 |

**We have grown Er:$CeO_2$ thin films with 2-130 ppm Er, each 740-940 nm thick.**



Grant et al, *APL Materials*, 12, 021121 (2024)

# Microstructural analysis of Er:$CeO_2$

THE UNIVERSITY OF CHICAGO
PRITZKER SCHOOL OF MOLECULAR ENGINEERING
Argonne NATIONAL LABORATORY
Q-NEXT NEXT GENERATION QUANTUM SCIENCE AND ENGINEERING


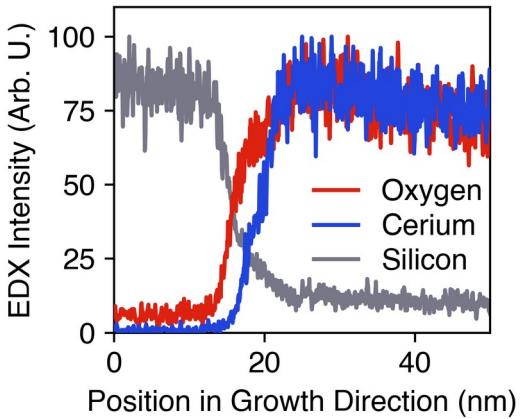


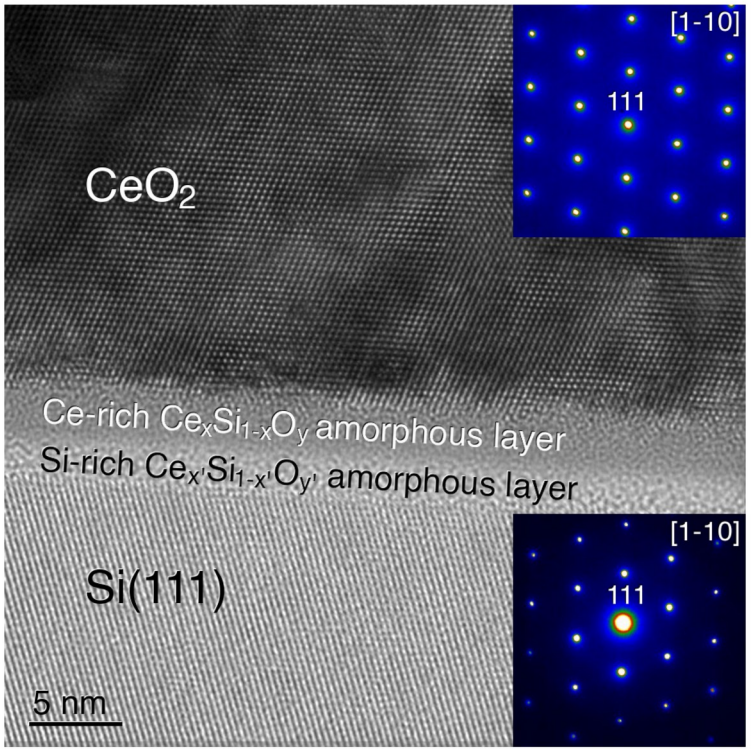


Lo-mag XTEM shows high concentration of threading dislocations, ~3 x $10^9$ per $cm^2$

Hi-mag XTEM shows good epitaxial registry, but an amorphous mixed-oxide bilayer confirmed by EDX



Grant et al, *APL Materials*, 12, 021121 (2024)

# Microstructural analysis of Er:$CeO_2$

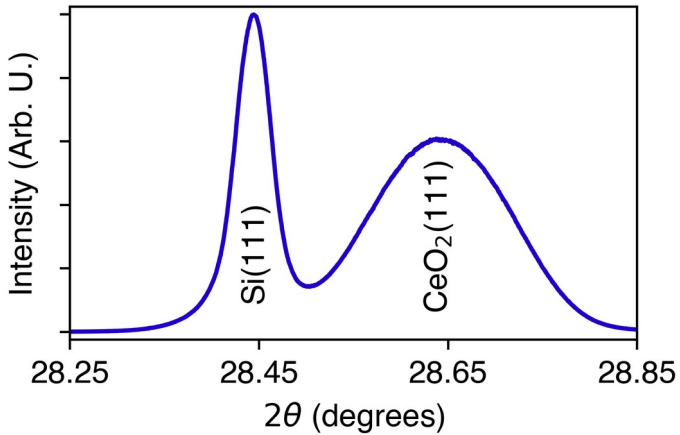


X-ray diffraction ω-2θ yields a $CeO_2$(111) peak near the Si(111) peak, with a=5.39 Å

$CeO_2$(111) peak width agrees with lo-mag TEM

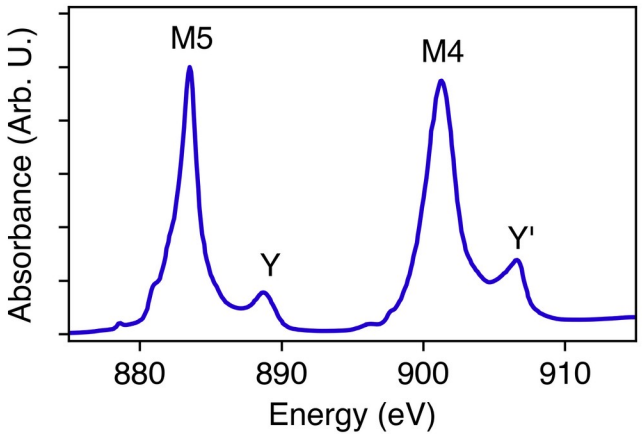


X-ray absorption $Ce^{4+}$ spectrum (not $Ce^{3+}$), confirming desired valency and therefore structure



Grant et al, *APL Materials*, 12, 021121 (2024)

# Confirming integration of Er into $CeO_2$

THE UNIVERSITY OF CHICAGO
PRITZKER SCHOOL OF MOLECULAR ENGINEERING
Argonne NATIONAL LABORATORY
Q-NEXT NEXT GENERATION QUANTUM SCIENCE AND ENGINEERING

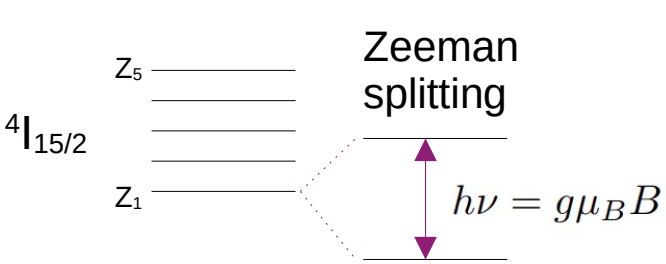


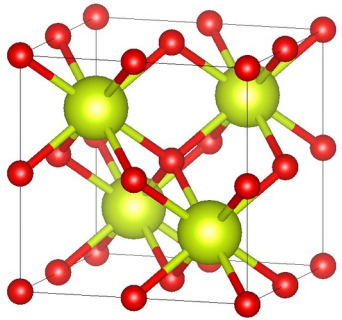

X-band electron paramagnetic resonance (EPR) of Er:$CeO_2$ at 3.5 K yields g-factor matching expected value for Er in a cubic $O_h$ site.

**g = 6.812 ± 0.001**

Hyperfine peak intensity matches natural abundance Er isotopes, and yields hyperfine splitting.

**A = 686.5 ± 1.3 MHz**

EPR resonance peaks of Er:$CeO_2$

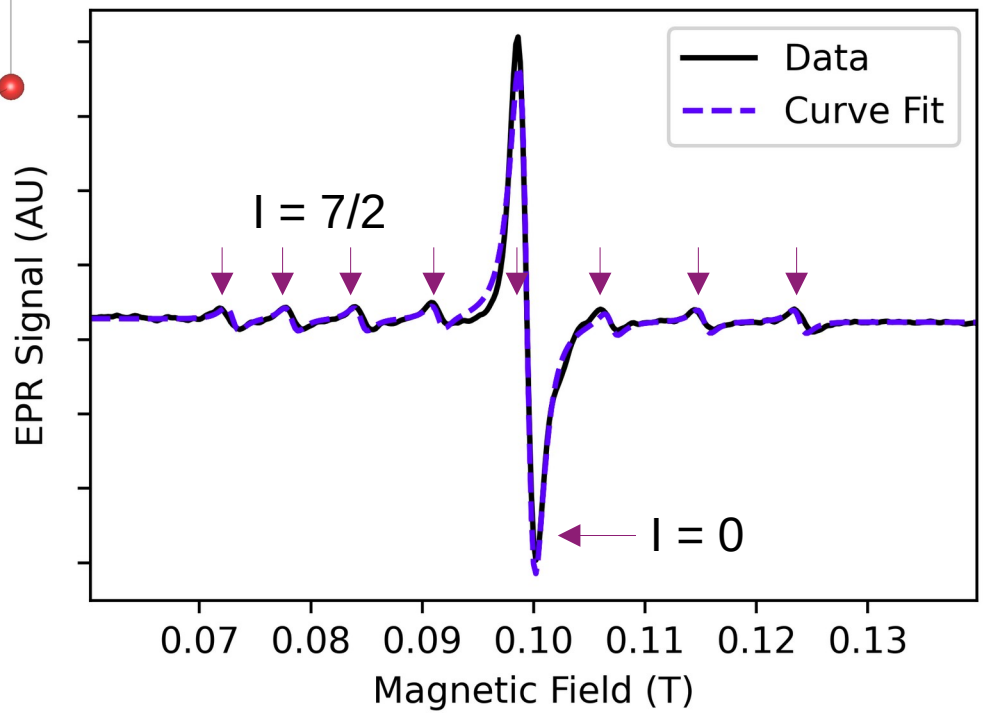




Grant et al, *APL Materials*, 12, 021121 (2024)

# Er-dependent spin linewidth broadening

THE UNIVERSITY OF CHICAGO
PRITZKER SCHOOL OF MOLECULAR ENGINEERING
Argonne NATIONAL LABORATORY
Q-NEXT NEXT GENERATION QUANTUM SCIENCE AND ENGINEERING

Grew Er:$CeO_2$ samples varied Er doping levels:
- All grown under the same conditions
- 2 ppm to 130 ppm
- Films between 740 and 940 nm thick

We track the linewidth of the spin resonance in EPR as a function of Er concentration.

Broadening observed in EPR linewidth is greater than Er-Er interactions alone. [1]

$$\Gamma_{\mathrm{EPR}} > \Gamma_{dd} = \frac{\pi}{9\sqrt{3}} \frac{\mu_0 (g\mu_B)^2}{h} C$$

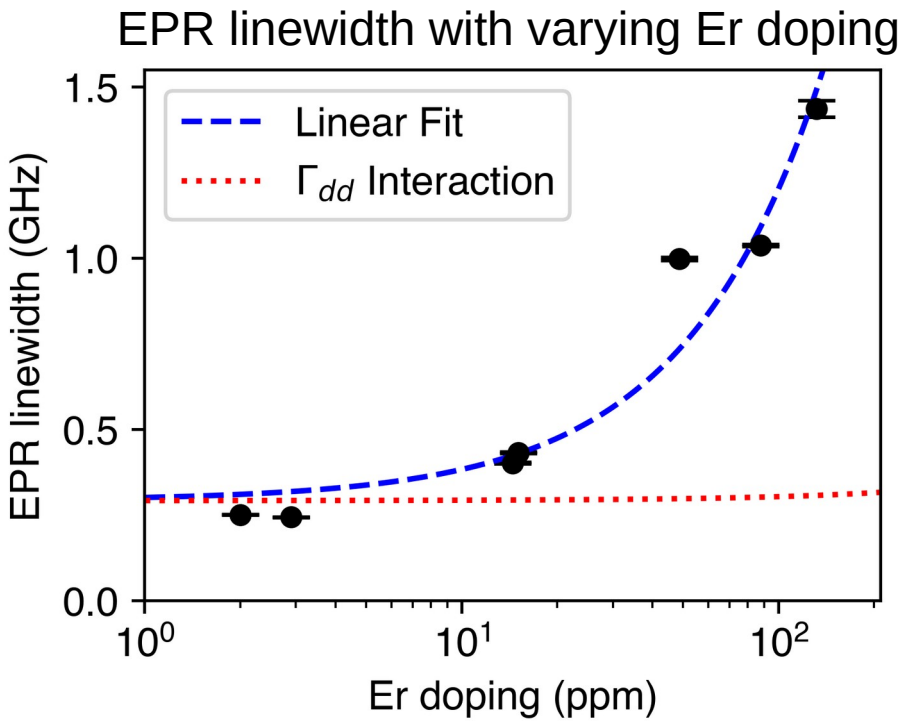




[1]: Geschwind, *Electron Paramagnetic Resonance* (1972)
Grant et al, *APL Materials*, 12, 021121 (2024)

# Setting up optical analysis of $Er:CeO_2$

THE UNIVERSITY OF CHICAGO
PRITZKER SCHOOL OF MOLECULAR ENGINEERING
Argonne NATIONAL LABORATORY
Q-NEXT NEXT GENERATION QUANTUM SCIENCE AND ENGINEERING

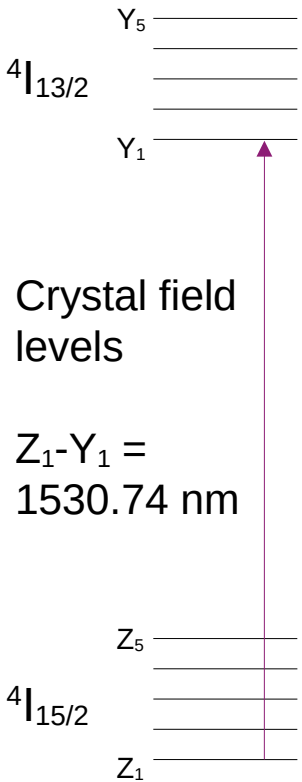


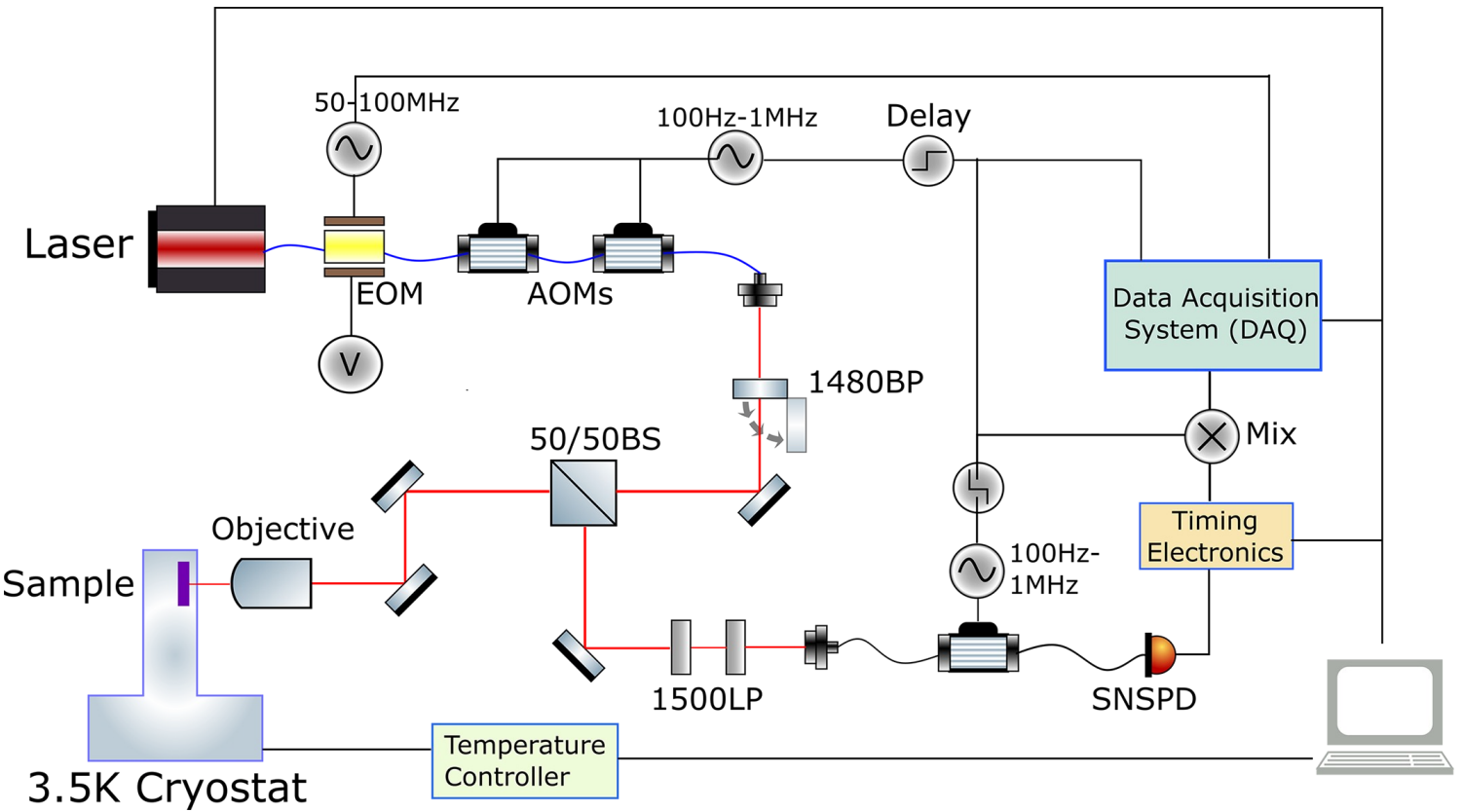




Zhang et al, arXiv:2309.16785 (2023)
Grant et al, *APL Materials*, 12, 021121 (2024)

# PL measurements of Er:$CeO_2$

THE UNIVERSITY OF CHICAGO
PRITZKER SCHOOL OF MOLECULAR ENGINEERING
Argonne NATIONAL LABORATORY
Q-NEXT NEXT GENERATION QUANTUM SCIENCE AND ENGINEERING

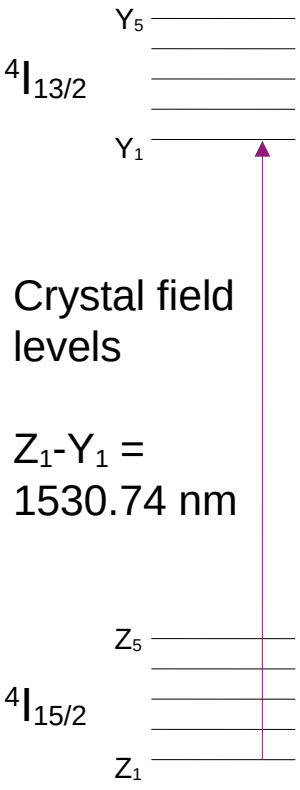


Crystal field levels

$Z_1$-$Y_1$ = 1530.74 nm

| $Er^{3+}$ Level | Crystal Field Level | Level Energy (meV) | Transition Wavelength to $Z_1$ (nm) | Transition Wavelength to $Y_1$ (nm) |
|---|---|---|---|---|
| $^4I_{13/2}$ | $Y_5$ | Not observed | – | |
| | $Y_4$ | 821.741 | 1508.8 | – |
| | $Y_3$ | 813.171 | 1524.7 | – |
| | $Y_2$ | 811.097 | 1528.6 | – |
| | $Y_1$ | 809.931 | 1530.7 | – |
| $^4I_{15/2}$ | $Z_5$ | Not observed | | – |
| | $Z_4$ | 5.517 | – | 1541.3 |
| | $Z_3$ | 3.188 | – | 1536.8 |
| | $Z_2$ | 1.479 | – | 1533.6 |
| | $Z_1$ | 0 | – | 1530.7 |

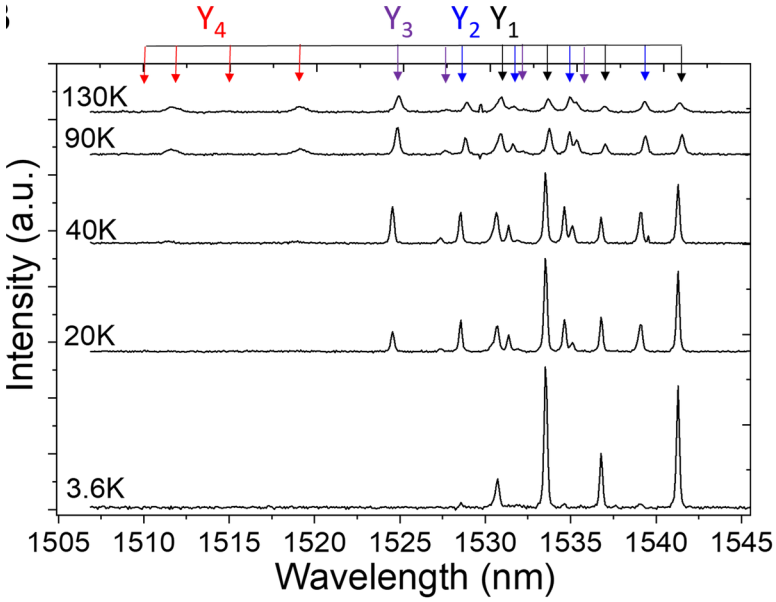


Raising sample temperature populates higher Z and Y levels, accessing new peaks in the PL spectrum.



Zhang et al, arXiv:2309.16785 (2023)

# PLE measurements of Er:$CeO_2$

THE UNIVERSITY OF CHICAGO
PRITZKER SCHOOL OF MOLECULAR ENGINEERING
Argonne NATIONAL LABORATORY
Q-NEXT NEXT GENERATION QUANTUM SCIENCE AND ENGINEERING

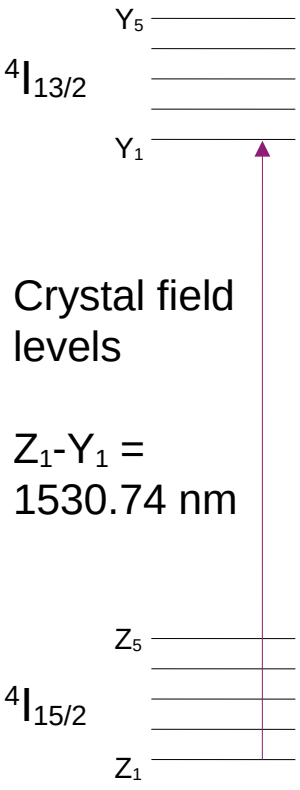


Crystal field levels

$Z_1$-$Y_1$ = 1530.74 nm

Example PLE measurement of a 15 ppm Er:$CeO_2$ sample:

Sample is illuminated for 1.5ms; emission is collected after that.

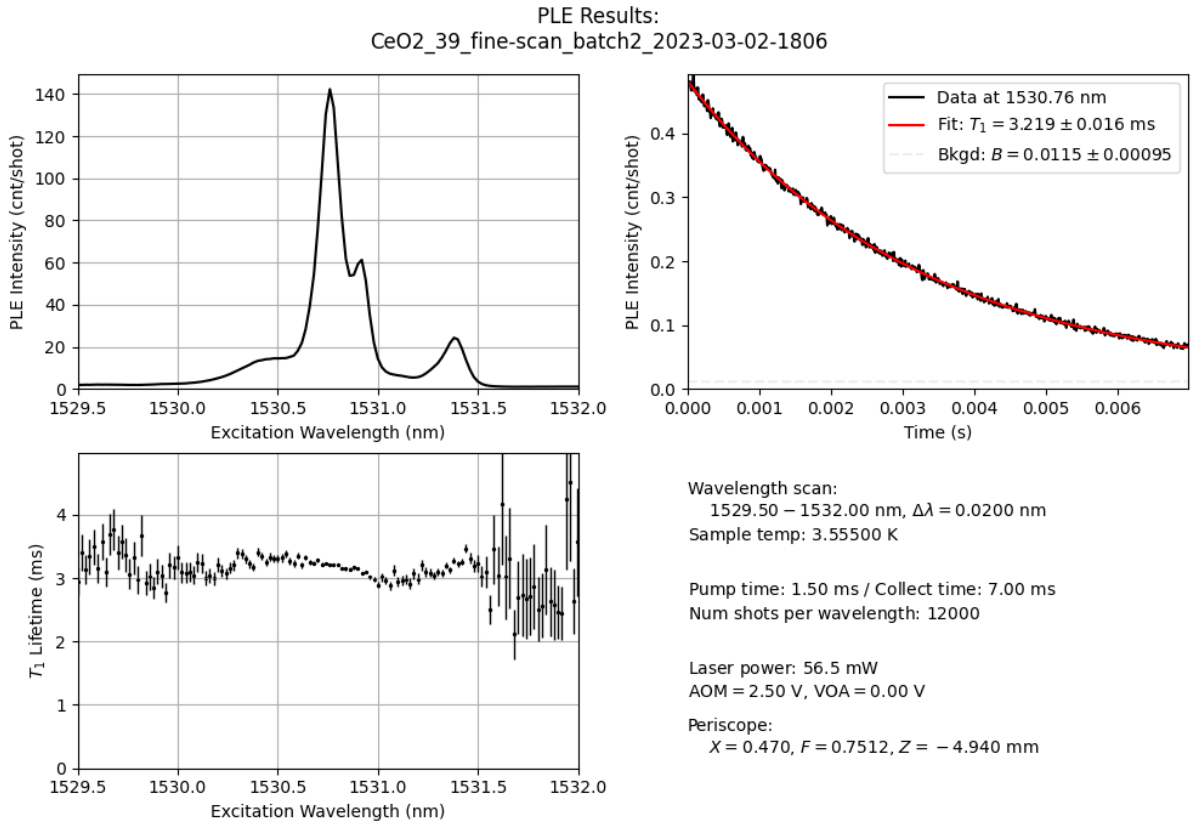




Grant et al, *APL Materials*, 12, 021121 (2024)

# $Z_1$-$Y_1$ PLE measurements of Er:$CeO_2$

Recall Er:$CeO_2$ doping series

THE UNIVERSITY OF CHICAGO
PRITZKER SCHOOL OF MOLECULAR ENGINEERING
Argonne NATIONAL LABORATORY
Q-NEXT NEXT GENERATION QUANTUM SCIENCE AND ENGINEERING

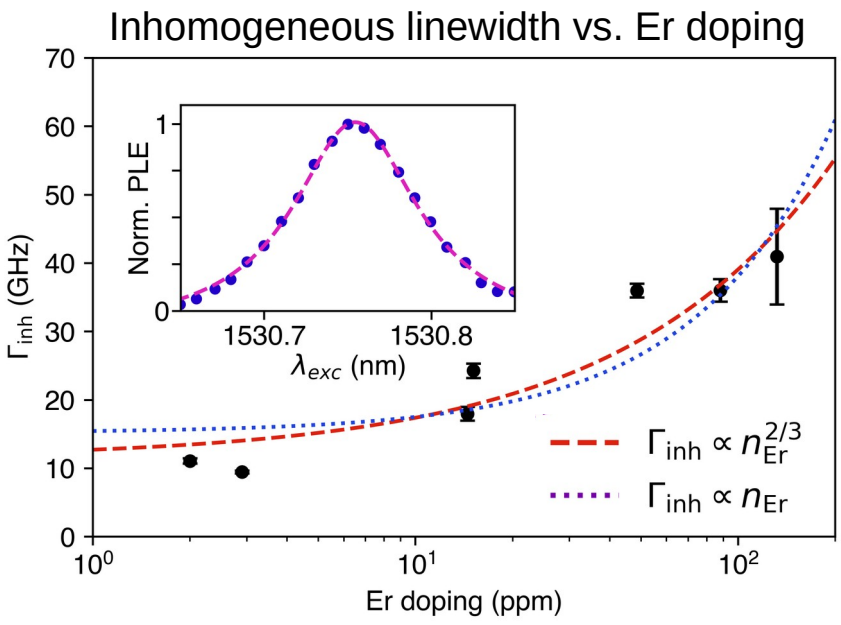


Broadening mechanisms via Stoneham [1]:
~$n^{2/3}$ : dipoles near charge defects
~$n^{1}$ : dipoles near dipoles, strain fields, or random electric fields

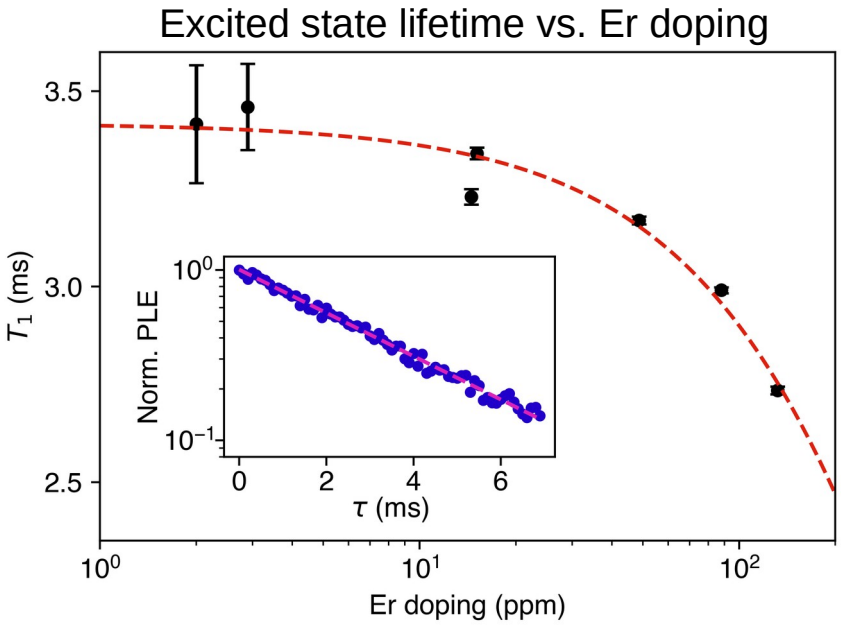


$T_1$ reduction matches Inokuti-Hirayama (I-H) theory of nearby quenching defects [2], with more defects allowing more decay pathways

[1]: Stoneham, *Rev. Mod. Phys.*, 41, 1 (1969)
[2]: Inokuti & Hirayama, *J. Chem. Phys.*, 43, 1978-89 (1965)
Grant et al, *APL Materials*, 12, 021121 (2024)

# $Z_1$-$Y_1$ spectral diffusion measurements

THE UNIVERSITY OF CHICAGO
PRITZKER SCHOOL OF MOLECULAR ENGINEERING
Argonne NATIONAL LABORATORY
Q-NEXT NEXT GENERATION QUANTUM SCIENCE AND ENGINEERING

Diagram of transient spectral holeburning (TSHB) laser illumination

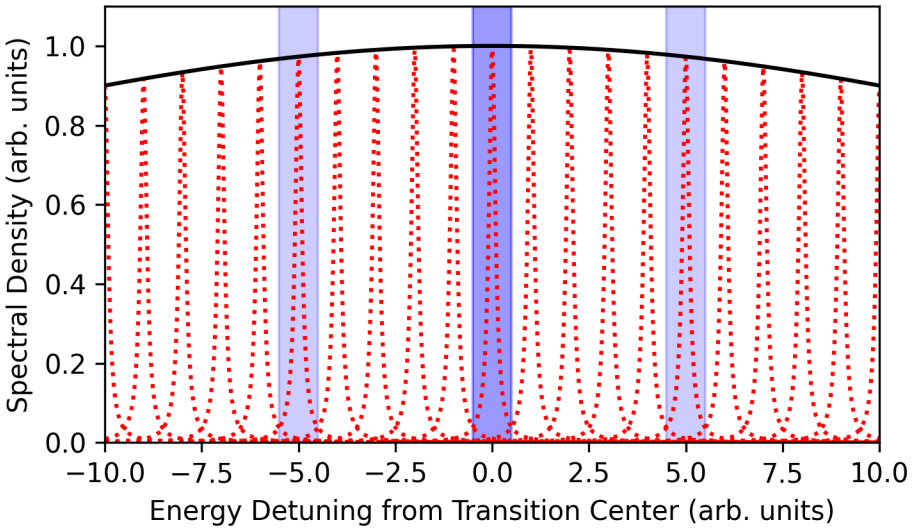


Laser sidebands are provided by a phase EOM placed prior to the AOMs

$$\Gamma_{\mathrm{hom}} \leq \Gamma_{\mathrm{TSHB}}/2$$

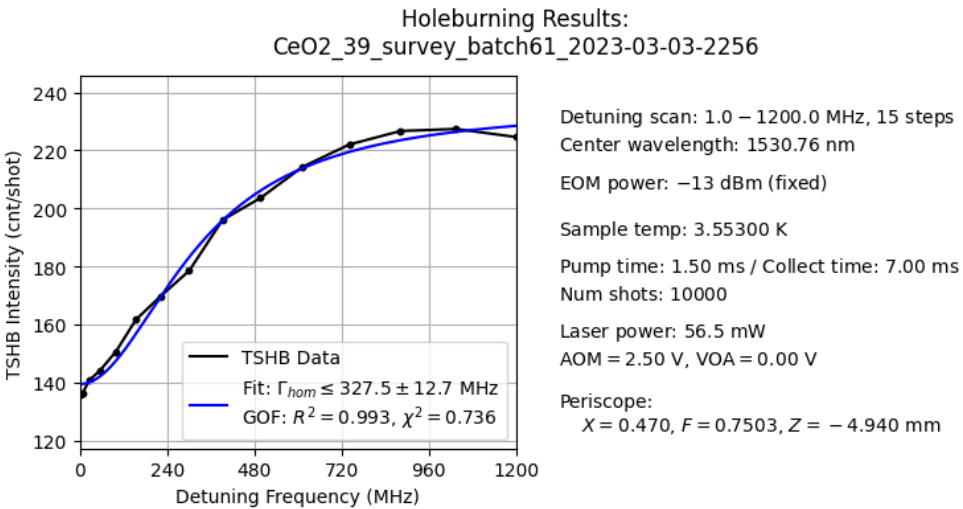


The resulting intensity profile yields the spectral diffusion linewidth, which bounds the homogeneous linewidth



Grant et al, *APL Materials*, 12, 021121 (2024)

# $Z_1$-$Y_1$ spectral diffusion measurements

THE UNIVERSITY OF CHICAGO
PRITZKER SCHOOL OF MOLECULAR ENGINEERING
Argonne NATIONAL LABORATORY
Q-NEXT NEXT GENERATION QUANTUM SCIENCE AND ENGINEERING

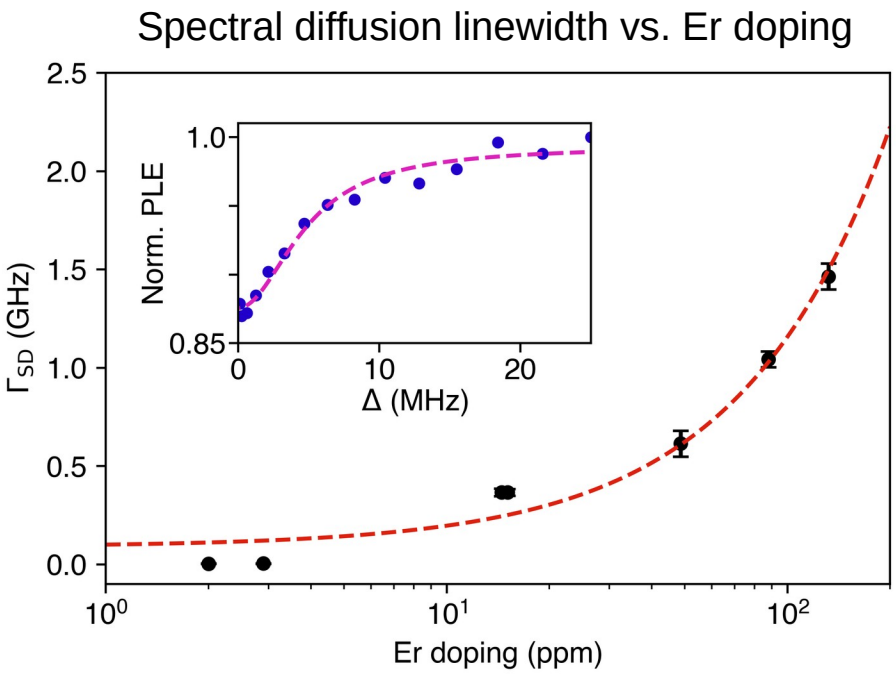


Spectral diffusion broadening is linear with increasing Er concentration.

This is consistent with instantaneous spectral diffusion (ISD) due to Er-Er interactions.

If we treat the minimum spectral diffusion linewidth of **5 MHz** as the worst-case homogeneous linewidth, then this implies a worst-case optical coherence time.

$$\mathbf{T_{2,opt} \geq 63\ ns}$$



Grant et al, *APL Materials*, 12, 021121 (2024)

# Improving optical properties via anneals

THE UNIVERSITY OF CHICAGO
PRITZKER SCHOOL OF MOLECULAR ENGINEERING
Argonne NATIONAL LABORATORY
Q-NEXT NEXT GENERATION QUANTUM SCIENCE AND ENGINEERING

Tested 12-hour 20% $O_2$/Ar anneals on a 200 nm thick, 3 ppm Er:$CeO_2$ film

Substituting $n_{Er}$ for a population of **thermally-annihilated defects** extends PLE models for inhomogeneous linewidth and $T_1$, with an activation energy of 0.65-0.75 eV.

Inhomogeneous linewidth narrows ~20% with 900 C

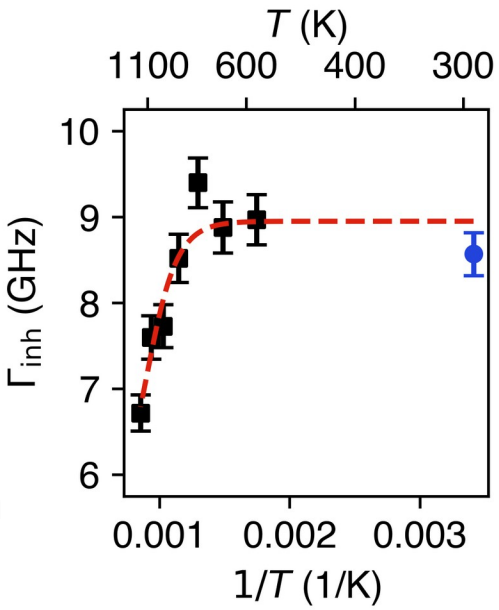


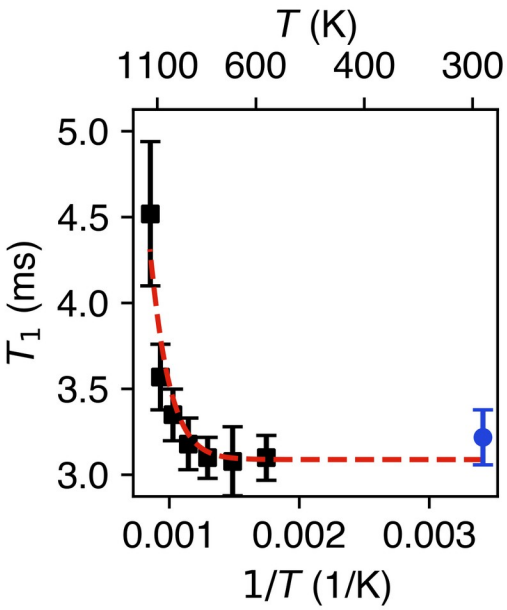


Excited state lifetime increases ~40% with 900 C

Spectral diffusion linewidth irregular with annealing

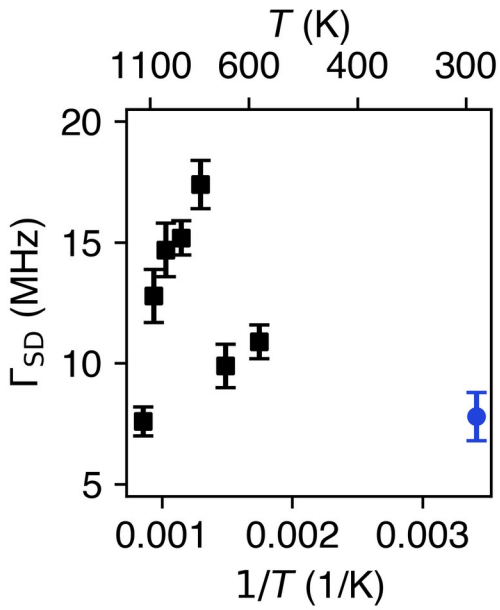




Grant et al, *APL Materials*, 12, 021121 (2024)

# Test for optical echo in Er:$CeO_2$

THE UNIVERSITY OF CHICAGO
PRITZKER SCHOOL OF MOLECULAR ENGINEERING
Argonne NATIONAL LABORATORY
Q-NEXT NEXT GENERATION QUANTUM SCIENCE AND ENGINEERING

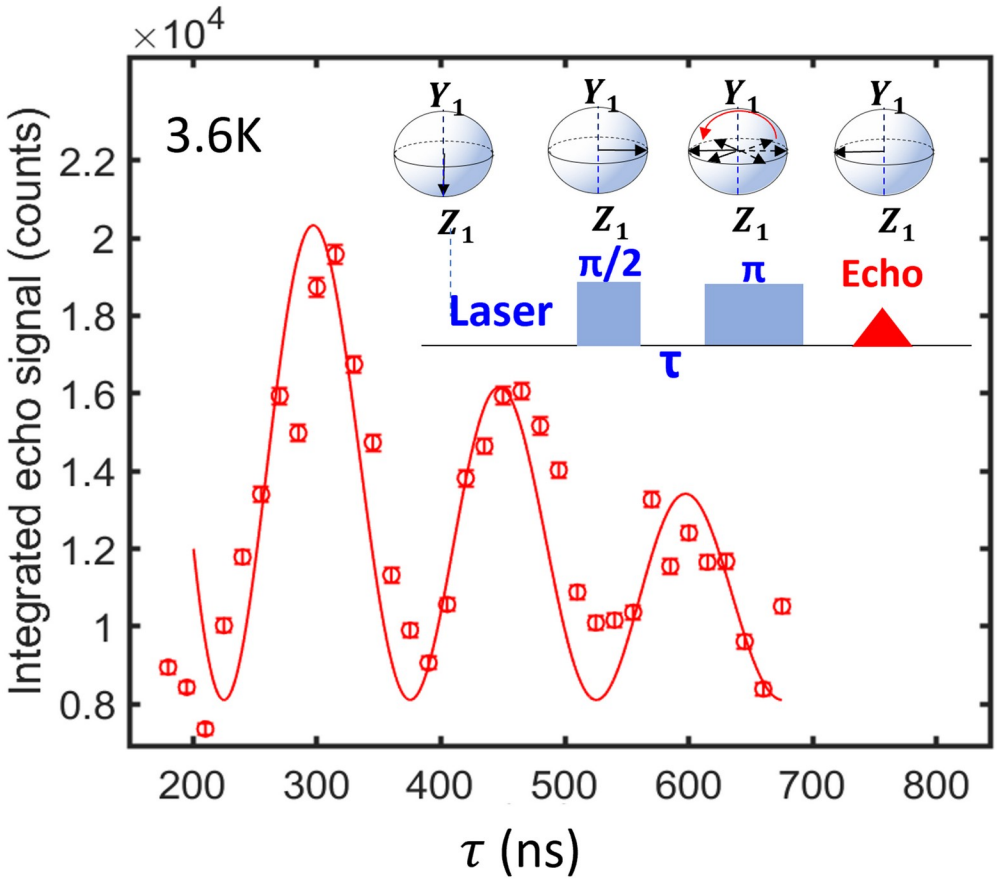


We may use photon echo to probe the homogeneous linewidth, knowing that we have $T_{2,opt}$ **≥ 63 ns** > ~50 ns.

We find a homogeneous linewidth of 440(20) kHz, or alternatively a **coherence time of $T_{2,opt}$ = 720(30) ns**.

Broadening dominated by Orbach relaxation at these temperatures (~4 K).

Coherent beating occurs with a frequency of ~3 MHz.

$$I(\tau) \propto \exp\{-4\tau/T_2\}$$

Zhang et al, arXiv:2309.16785 (2023)

# Test for spin echo in $Er:CeO_2$

THE UNIVERSITY OF CHICAGO
PRITZKER SCHOOL OF MOLECULAR ENGINEERING
Argonne NATIONAL LABORATORY
Q-NEXT NEXT GENERATION QUANTUM SCIENCE AND ENGINEERING

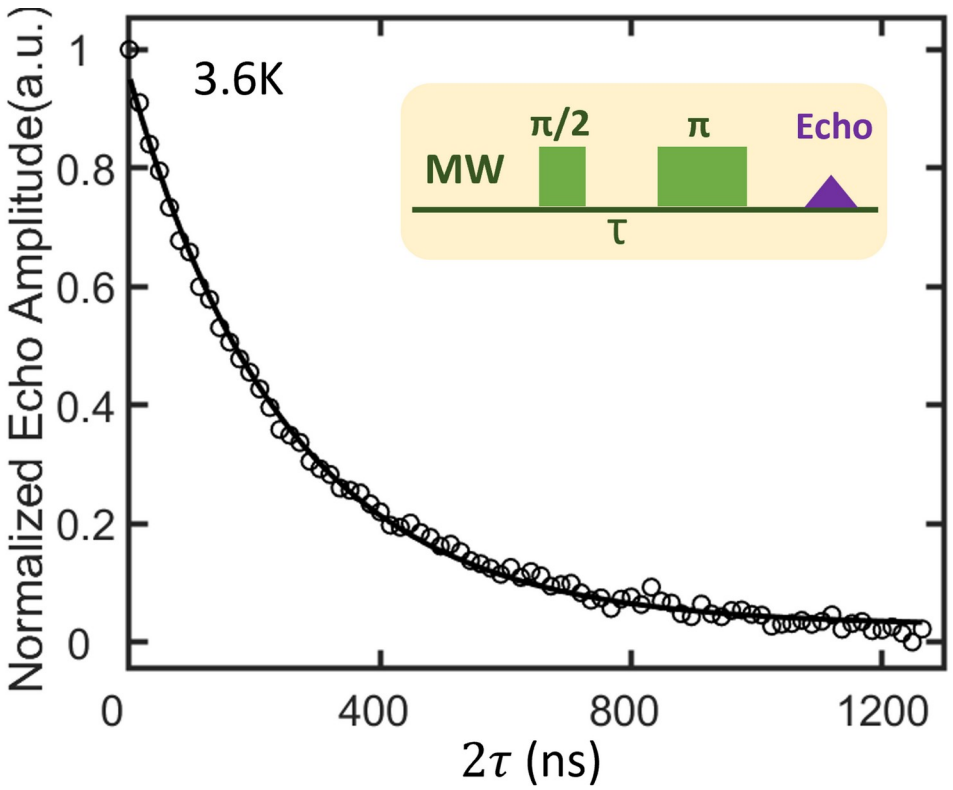


We may use spin echo to probe the coherence time of the spin transition as well.

Via spin (Hahn) echo, we find a **coherence time of $T_{2,spin}$ = 249(35) ns**.

(No coherent beating occurs here.)

$$I(\tau) \propto \exp\{-2\tau/T_2\}$$



Zhang et al, arXiv:2309.16785 (2023)

# Using spin echo to get spin lifetime

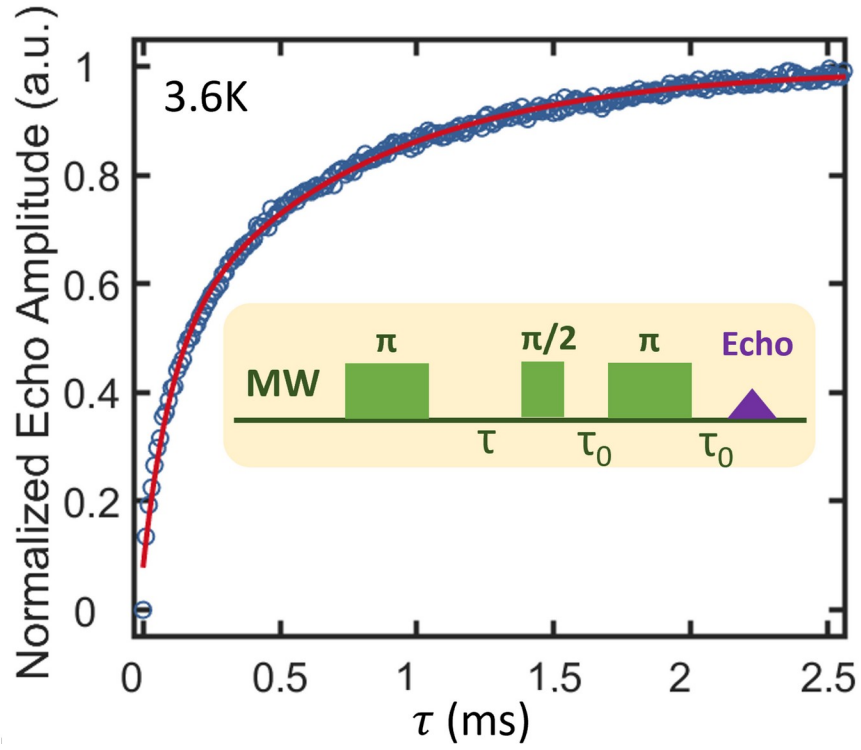


Prepending a pulse to the spin echo sequence gives us inversion recovery, which yields the spin lifetime as well.

Via inversion recovery, we find a double relaxation processes with spin lifetimes of:

$T_{1,spin,A}$ = 0.11(1) ms

**$T_{1,spin,B}$ = 0.83(4) ms**

Optical measurements confirm the B process here is the lifetime of the spin split states in $Z_1$.



Zhang et al, arXiv:2309.16785 (2023)

# Summary of Er:$CeO_2$ benchmarking

THE UNIVERSITY OF CHICAGO
PRITZKER SCHOOL OF MOLECULAR ENGINEERING
Argonne NATIONAL LABORATORY
Q-NEXT NEXT GENERATION QUANTUM SCIENCE AND ENGINEERING

Er:$CeO_2$ provides a promising quantum memory platform at 3.5 K, particularly at low doping levels of 2-3 ppm Er.

EPR yields g = 6.81 ± 0.01, A = 687 ± 1 MHz
PLE of optical $Z_1$-$Y_1$ demonstrates, for as-grown samples:
$\Gamma_{inh}$ = 9.5 ± 0.2 GHz
$T_{1,opt}$ = 3.5 ± 0.1 ms

Oxygen anneals provide modest improvements to inhomogeneous linewidth and excited state lifetimes.

**Spin echo and photon echo yield coherence times:**
**$T_{2,spin}$ = 0.25 ± 0.04 µs**
**$T_{2,optical}$ = 0.72 ± 0.03 µs**

Next steps:
- Measurement at mK temperatures to identify coherence limits
- Nanophotonics cavities for **Er:$CeO_2$ on SOI**, to enhance $Z_1$-$Y_1$
- Lower Er doping to saturate $\Gamma_{inh}$, $T_1$, and $T_2$ lower bounds

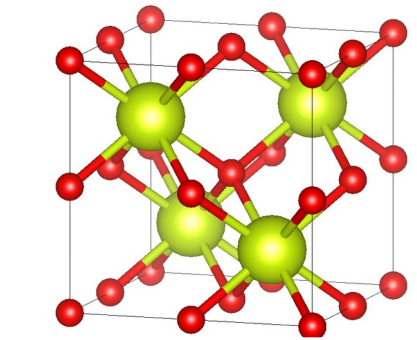

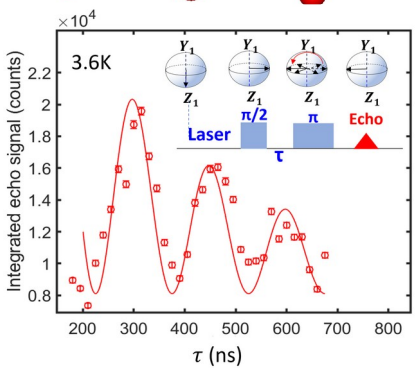


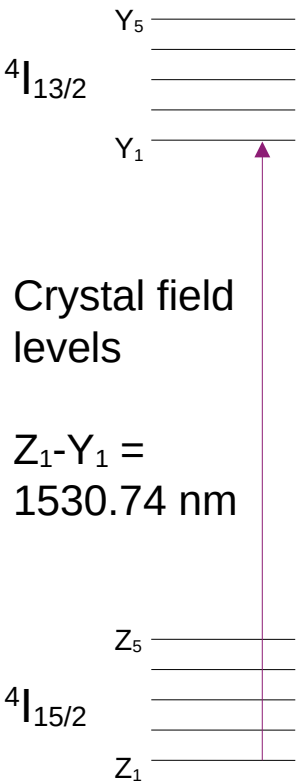


**Grant et al, *APL Materials*, 12, 021121 (2024)**
**Zhang et al, arXiv:2309.16785 (2023);**
**in review with npjQI**

# Thesis Defense Outline



1. Discussion on selecting a quantum communication-relevant defect
2. Review of erbium energy structure and aspects relevant to our work
3. Developing $CeO_2$ as a host for Er
4. **Expanding $CeO_2$ to other substrates for alternative integrations**
5. Considering other host materials for Er via computational survey
6. Conclusions and final remarks

# Silicon substrate orientations

THE UNIVERSITY OF CHICAGO
PRITZKER SCHOOL OF MOLECULAR ENGINEERING
Argonne NATIONAL LABORATORY
Q-NEXT NEXT GENERATION QUANTUM SCIENCE AND ENGINEERING

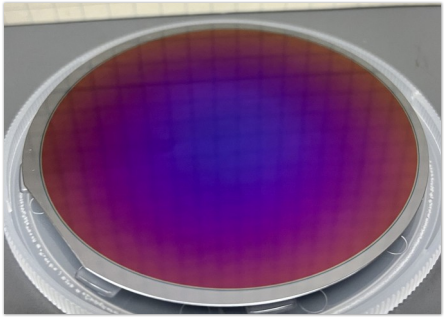

Films may be grown on different substrate orientations.

Different orientations yields different growth behavior.
Most semiconductor fabrication is on Si(001).

Si unit cell

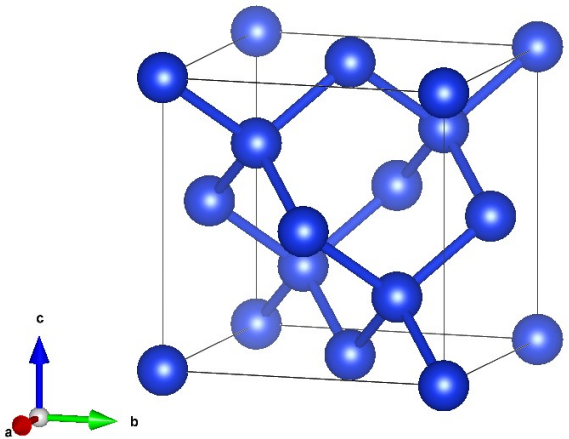


Si(001)

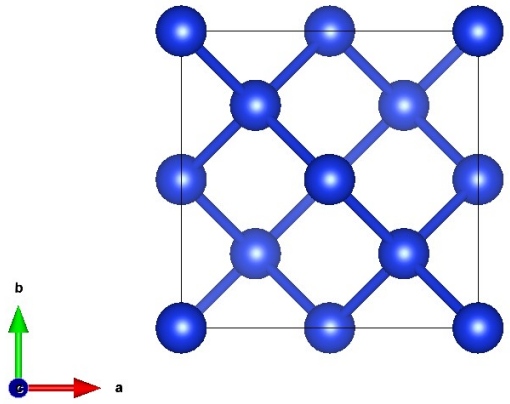


Si(111)

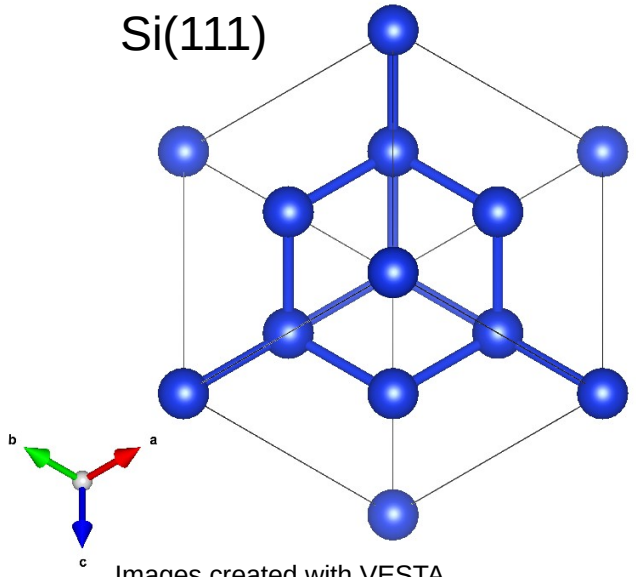


Images created with VESTA
*Manuscript in preparation*

# Growing Er:$CeO_2$ via MBE on (001)

THE UNIVERSITY OF CHICAGO
PRITZKER SCHOOL OF MOLECULAR ENGINEERING
Argonne NATIONAL LABORATORY
Q-NEXT NEXT GENERATION QUANTUM SCIENCE AND ENGINEERING

Molecular beam epitaxy (MBE) recipe:

1. Start with base growth chamber pressure of $10^{-9}$ torr
2. Clean substrate
   - Si = RCA cleaned, HF last
   - $SrTiO_3$ (STO) = Acetone + IPA sonication
3. Prep substrate for growth
   - Si = Flash to 4x surface reconstruction
   - STO = 20 minutes plasma clean
4. Evaporate high-purity cerium and erbium metal; flow oxygen

Attempted four growths, all with 10 ppm Er and grown at 50-70 nm/hr:

- On Si(111), 670 $^oC$ substrate
- On STO(001), 670 $^oC$ substrate
- On Si(001), 670 $^oC$ substrate
- On Si(001), room temperature substrate

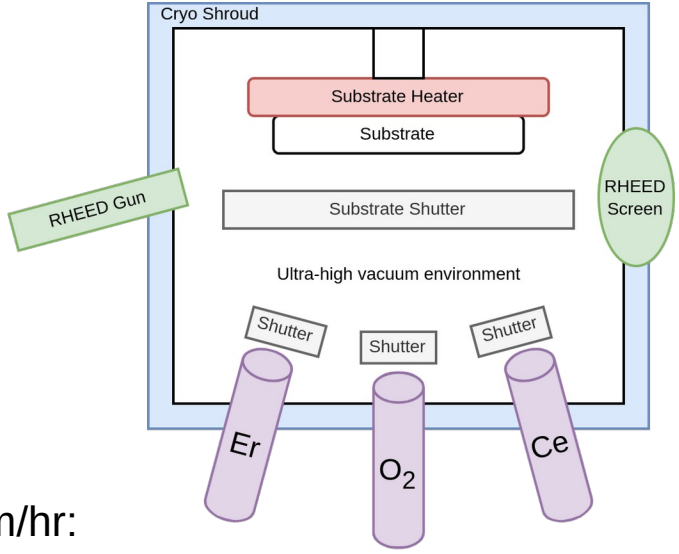


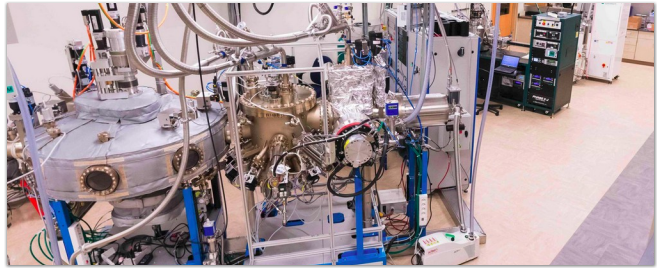

*Manuscript in preparation*

# Si(111) and STO yield epitaxial growth

THE UNIVERSITY OF CHICAGO
PRITZKER SCHOOL OF MOLECULAR ENGINEERING
Argonne NATIONAL LABORATORY
Q-NEXT NEXT GENERATION QUANTUM SCIENCE AND ENGINEERING

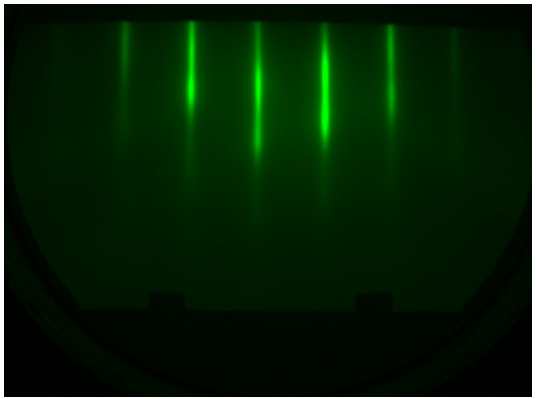

$CeO_2$(111) on Si(111)

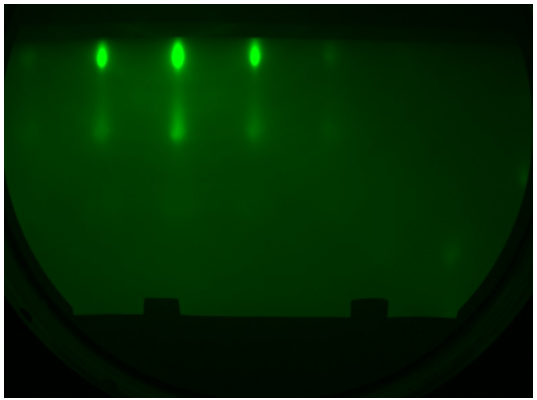

$CeO_2$(001) on STO(001), along STO<110> azimuth

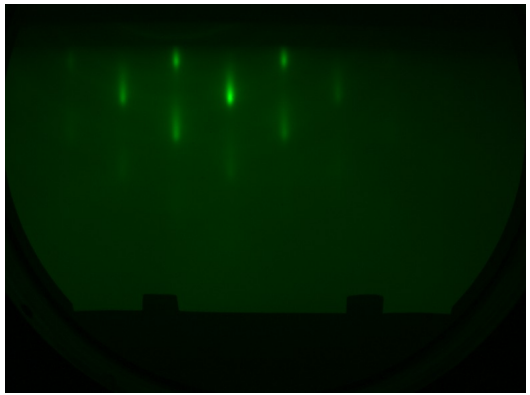

$CeO_2$(001) on STO(001), along STO<100> azimuth

These streaky patterns indicate single-crystalline, epitaxial growth.

The “standard” recipe developed for $CeO_2$ on Si(111) can work when growing $CeO_2$(001).



*Manuscript in preparation*

# Si(001) yields subdivisions in $CeO_2$ films

THE UNIVERSITY OF CHICAGO
PRITZKER SCHOOL OF MOLECULAR ENGINEERING
Argonne NATIONAL LABORATORY
Q-NEXT NEXT GENERATION QUANTUM SCIENCE AND ENGINEERING

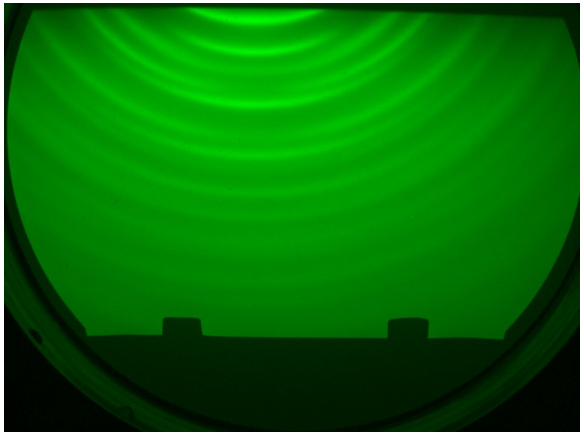

Poly $CeO_2$ on Si(001), grown at room temp

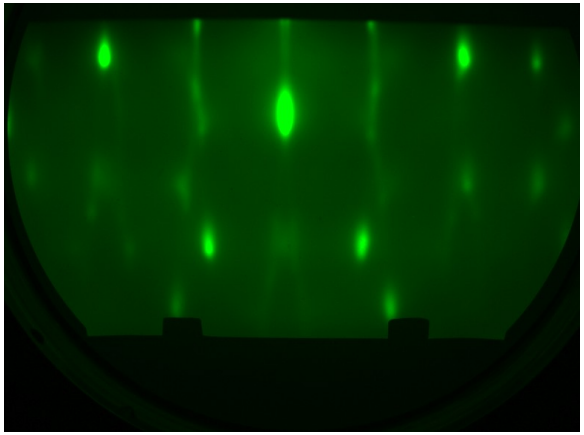

CeO2 on Si(001), along Si<100> azimuth

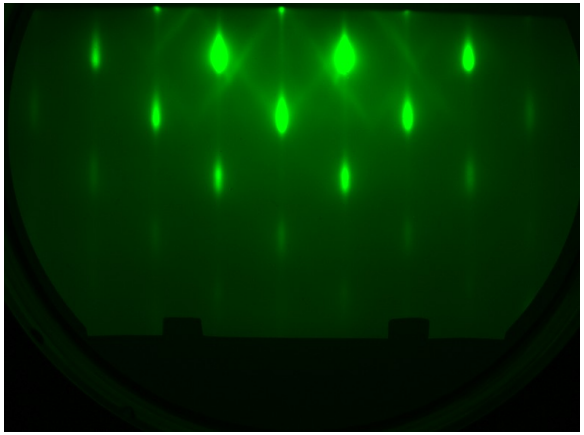

CeO2 on Si(001), along Si<110> azimuth

Room temperature growth yields polycrystalline $CeO_2$.

Standard growth conditions on Si(001) yields oddly partitioned streaky RHEED, with streak spacing matching either $CeO_2$(001) or $CeO_2$(011) growth.



*Manuscript in preparation*

# SEM and XRD of $CeO_2$ on Si(001)

THE UNIVERSITY OF CHICAGO
PRITZKER SCHOOL OF MOLECULAR ENGINEERING
Argonne NATIONAL LABORATORY
Q-NEXT NEXT GENERATION QUANTUM SCIENCE AND ENGINEERING


SEM shows small cross-hatched domains, indicating twinning

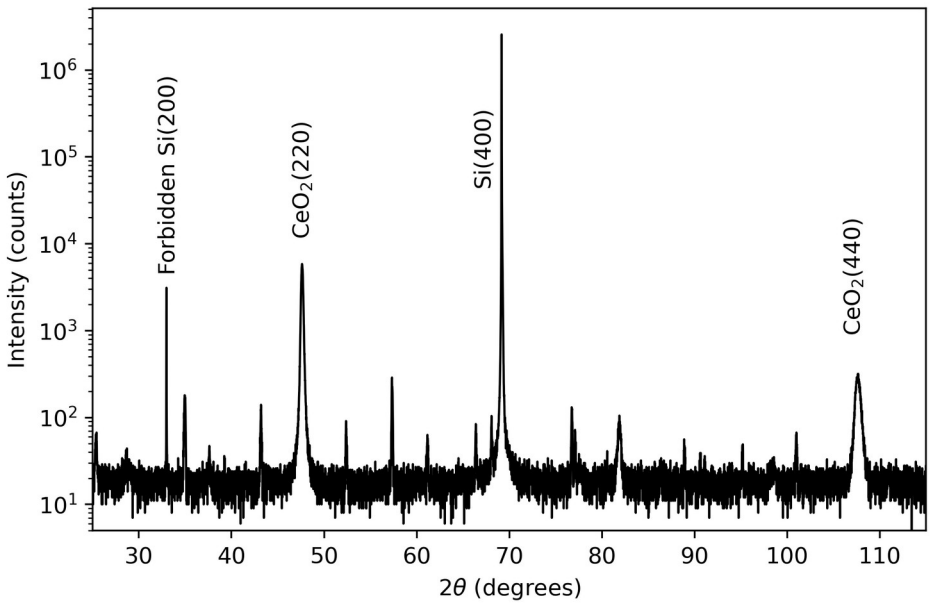


XRD shows $CeO_2$(220) and $CeO_2$(440) peaks, so we have $CeO_2$(110) growth on Si(001).



*Manuscript in preparation*

# How are optical properties on Si(001)?

THE UNIVERSITY OF CHICAGO
PRITZKER SCHOOL OF MOLECULAR ENGINEERING
Argonne NATIONAL LABORATORY
Q-NEXT NEXT GENERATION QUANTUM SCIENCE AND ENGINEERING

| Substrate | Growth Info | RHEED Pattern | $\Gamma_{inh}$ (GHz) | $T_1$ (ms) | $\Gamma_{SD}$ (MHz) |
|---|---|---|---|---|---|
| Si(001) | Room-temp | Poly rings | No signal | – | – |
| Si(111) | Standard | Single streaks | $16.8 \pm 1.1$ | $3.6 \pm 0.1$ | $328 \pm 13$ |
| Si(001) | Standard | Multi streaks | $28.9 \pm 3.5$ | $3.8 \pm 0.1$ | $450 \pm 8$ |
| STO(001) | Standard | Single streaks | $28.2 \pm 0.3$ | $5.3 \pm 0.2$ | $397 \pm 7$ |

We make the following observations for Er:$CeO_2$ grown on Si(001):
- Room temperature growth results in no activated Er
- Linewidths worsen when moving from Si(111) to Si(001)
- Linewidths on STO(001) and Si(001) are comparable despite multiple domains

Next steps:
- Optimize $CeO_2$(001) growth window on STO(001)
- Investigate buffer layers for $CeO_2$(001) on Si(001), such as STO
- Investigate if roughness of $CeO_2$(011) films is low enough fabrication



*Manuscript in preparation*

# Thesis Defense Outline



1. Discussion on selecting a quantum communication-relevant defect
2. Review of erbium energy structure and aspects relevant to our work
3. Developing $CeO_2$ as a host for Er
4. Expanding $CeO_2$ to other substrates for alternative integrations
5. **Considering other host materials for Er via computational survey**
6. Conclusions and final remarks

# Shortening optical lifetimes of $Er^{3+}$

THE UNIVERSITY OF CHICAGO
PRITZKER SCHOOL OF MOLECULAR ENGINEERING
Argonne NATIONAL LABORATORY
Q-NEXT NEXT GENERATION QUANTUM SCIENCE AND ENGINEERING

Speeding up rare-earth emission would yield easier characterization measurements (e.g., PLE, $g^{(2)}$), and eventually **higher quantum communication bandwidth**.

## Option 1: Modify the local density of states

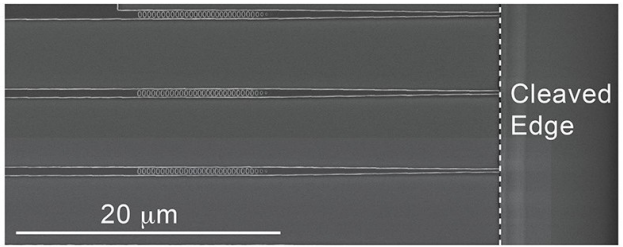


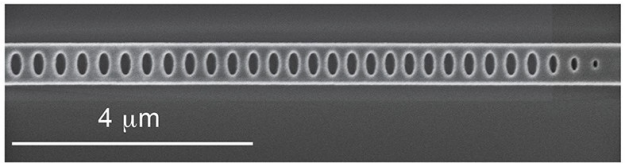


Nanophotonic devices, under development per, e.g., Alan Dibos' work.

## Option 2: Modify the available energy transitions

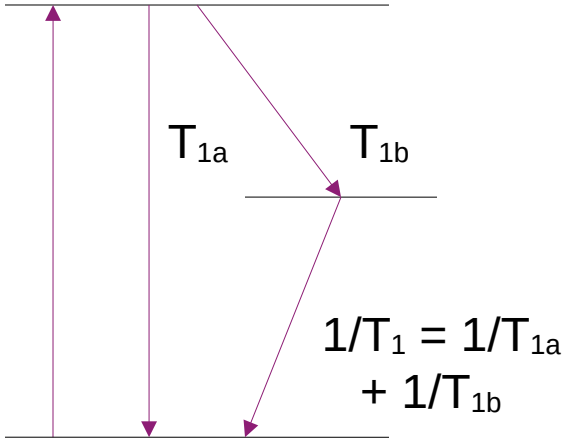


Adding defects yields extra relaxation channels (I-H theory). But, defects like this reduce photon yield and coherence.

## Option 3: Modify the intrinsic transition relaxation rate

$$\frac{1}{T_1} \propto \left|\langle f| \boldsymbol{P} |i\rangle\right|^2$$

The transition relaxation rate increases as the matrix element of the transition operator **P** increases. This matrix element depends on the host environment.

Electric dipole transitions **P**=e**r** are allowed if the initial and final states have different parity.

# Parity mixing yields visible $Er^{3+}$

THE UNIVERSITY OF CHICAGO
PRITZKER SCHOOL OF MOLECULAR ENGINEERING
Argonne NATIONAL LABORATORY
Q-NEXT NEXT GENERATION QUANTUM SCIENCE AND ENGINEERING

Rare-earth free-ion states have the same parity when in the same configuration, causing forbidden electric dipole transitions (Ex: 4f-4f).

$$\int_{-\infty}^{\infty} \psi_f(r) r \psi_i(r) dr = 0$$

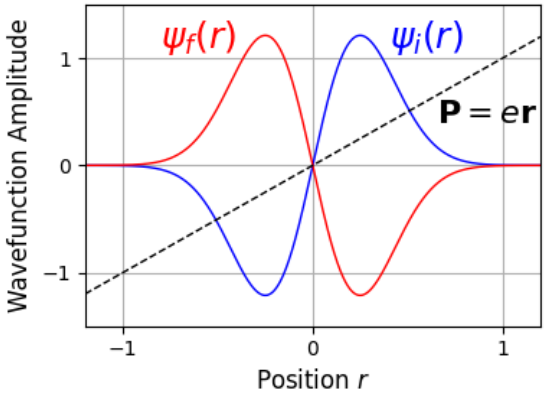


Electric dipole transitions are allowed if the initial and final states have different parity.

$$\int_{-\infty}^{\infty} \psi_f(r) r \psi_i(r) dr \approx 0.2$$

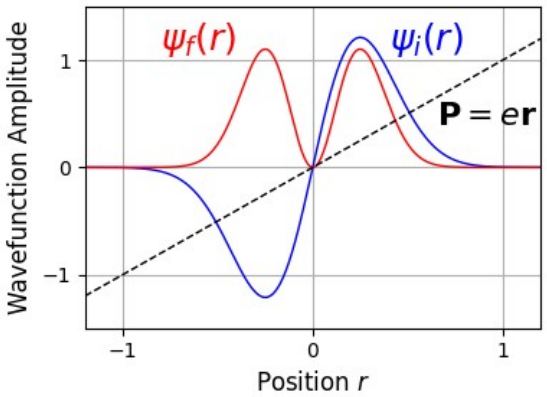


The **host crystal field** admixes higher states of **different parity** into the 4f states, weakly allowing electric dipole transitions.

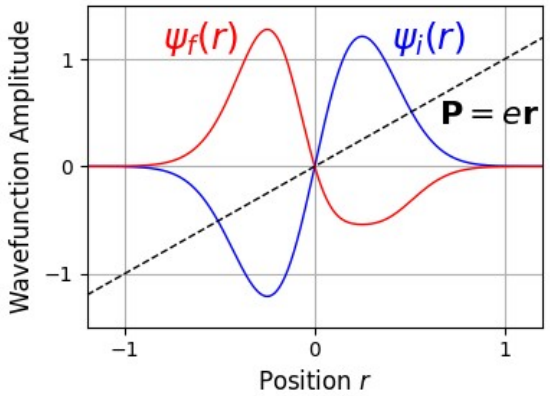


$$\int_{-\infty}^{\infty} \psi_f(r) r \psi_i(r) dr \approx 0.05$$

# $T_1$ from electric dipole transition

THE UNIVERSITY OF CHICAGO
PRITZKER SCHOOL OF MOLECULAR ENGINEERING
Argonne NATIONAL LABORATORY
Q-NEXT NEXT GENERATION QUANTUM SCIENCE AND ENGINEERING

Our goal is "brighter" Er from the $^4I_{13/2}$ to $^4I_{15/2}$ transition, defined by shorter $T_1$ excited state lifetimes in the $^4I_{13/2}$ states.

Calculating $T_1$ values:

1. Get $T_1$ by calculating the oscillator strength $f$.
2. Get $f$ from the electric dipole operator matrix element $D$
3. Get $D$ from the host crystal structure + Er structure

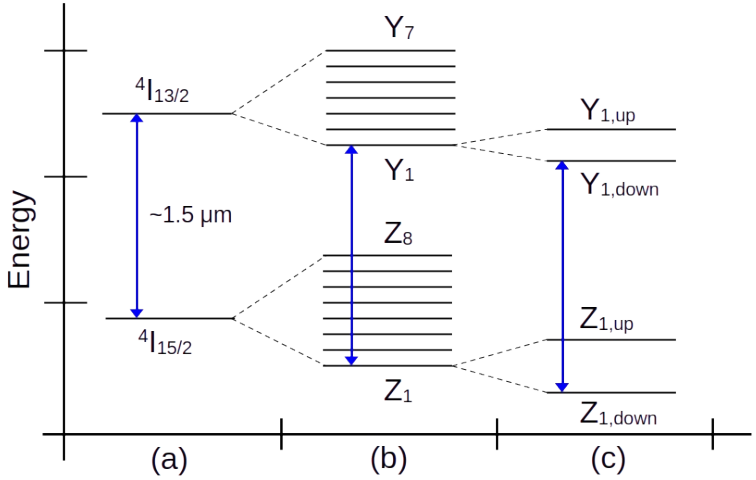


List of variables:

A = emission Einstein coefficient
$g_1$ = ground state degeneracy
$g_2$ = excited state degeneracy
ω = transition frequency
e = electron charge
$\epsilon_0$ = vacuum permittivity
$m_e$ = electron mass
c = speed of light
n = refractive index
h = Planck constant
J = ground state total ang. mom.

$$\frac{1}{T_1} = A = \frac{g_1}{g_2}\frac{\omega^2 e^2}{2\pi\epsilon_0 m_e c^3} f$$

$$f = \frac{(n^2+2)^2}{9n}\frac{8\pi^2 m_e c}{3h(2J+1)}|D|^2$$

# Clarifying the matrix element evaluation



The matrix element of the dipole operator ($D_\rho^{(1)} \sim r$) is evaluated in the perturbed basis B, when transitioning from state B to state B' [1]:

$$(1): \quad \langle B| D_\rho^{(1)} |B'\rangle = \sum_{k,q,\ \text{even}\ \lambda} (2\lambda+1)(-1)^{q+\rho} A_q^{(k)} \begin{pmatrix} 1 & \lambda & k \\ \rho & -q-\rho & q \end{pmatrix} \langle A| U_{q+\rho}^{(\lambda)} |A'\rangle \, \Xi(k,\lambda)$$

We then compute the connection between the unperturbed states A and A'. The summation may be then be rephrased to clarify the role of different terms.

$$(2): \quad \langle B| D_\rho^{(1)} |B'\rangle = \sum_{k,q,\ \text{even}\ \lambda} (2\lambda+1)(-1)^{q+\rho} A_q^{(k)} \begin{pmatrix} 1 & \lambda & k \\ \rho & -q-\rho & q \end{pmatrix} \langle A| U_{q+\rho}^{(\lambda)} |A'\rangle \, \Xi(k,\lambda)$$

$$\langle B| D_\rho^{(1)} |B'\rangle = \sum_{k,q} A_q^{(k)} \times \Big[ \sum_{\text{even}\ \lambda} (2\lambda+1)(-1)^{q+\rho} \begin{pmatrix} 1 & \lambda & k \\ \rho & -q-\rho & q \end{pmatrix} \langle A| U_{q+\rho}^{(\lambda)} |A'\rangle \, \Xi(k,\lambda) \Big]$$

And with this re-contextualization we can define **a new summation that is the element-wise multiplication of an Er-specific set of constants with the crystal field coefficients**.

$$(3): \quad \langle B| D_\rho^{(1)} |B'\rangle = \sum_{k,q} A_q^{(k)} \lambda_{kq,\rho} \ , \qquad \lambda_{kq,\rho} = \sum_{\text{even}\ \lambda} (2\lambda+1)(-1)^{q+\rho} \begin{pmatrix} 1 & \lambda & k \\ \rho & -q-\rho & q \end{pmatrix} \langle A| U_{q+\rho}^{(\lambda)} |A'\rangle \, \Xi(k,\lambda)$$



[1]: Judd, *Physical Review*, 1962.

# Computing the crystal field coefficients

THE UNIVERSITY OF CHICAGO
PRITZKER SCHOOL OF MOLECULAR ENGINEERING
Argonne NATIONAL LABORATORY
Q-NEXT NEXT GENERATION QUANTUM SCIENCE AND ENGINEERING

The crystal field coefficients $A_q^{(k)}$ arise from the expansion of a spatially-varying potential in the spherical harmonics.

$$H_3 = \sum_{k,q} A_q^{(k)} r^k C_q^{(k)}(\theta, \phi)$$

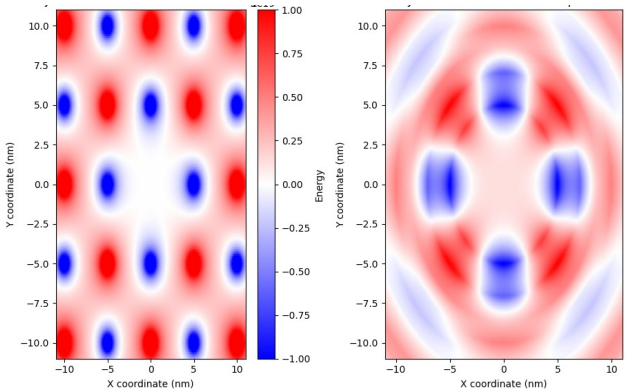


Recall:

$$\langle B| D_\rho^{(1)} |B'\rangle = \sum_{k,q} A_q^{(k)} \lambda_{kq,\rho}$$

$$C_q^{(k)} = \left(\frac{4\pi}{2k+1}\right)^{1/2} Y_{kq}$$

Hutchings (1964) [1] and Wybourne (1965) [2] provide an analytical solution for getting $A_{kq}$ from a field of point charges.

The crystal field potential upon an evaluation charge $Q_e$ caused by a field of ions with charge $Q_i$ at locations $\mathbf{R}_i$ is expanded in terms of the spherical harmonics $C_q^{(k)}$, yielding the crystal field coefficients $A_q^{(k)}$.

$$A_q^{(k)} = \frac{1}{4\pi\epsilon_0} \sum_i \frac{Q_e Q_i}{R_i^{k+1}} (-1)^q C_{-q}^{(k)}(\Theta_i, \Phi_i)$$

(This solution assumes no charge density of $Q_i$ coming within the $Er^{3+}$ electron radial wavefunctions.)



[1]: Hutchings, *Solid State Physics*, 1964.
[2]: Wybourne, "*Spect. Prop. of Rare Earths,*" 1965

# Workflow from Materials Project to |D|

THE UNIVERSITY OF CHICAGO
PRITZKER SCHOOL OF MOLECULAR ENGINEERING
Argonne NATIONAL LABORATORY
Q-NEXT NEXT GENERATION QUANTUM SCIENCE AND ENGINEERING

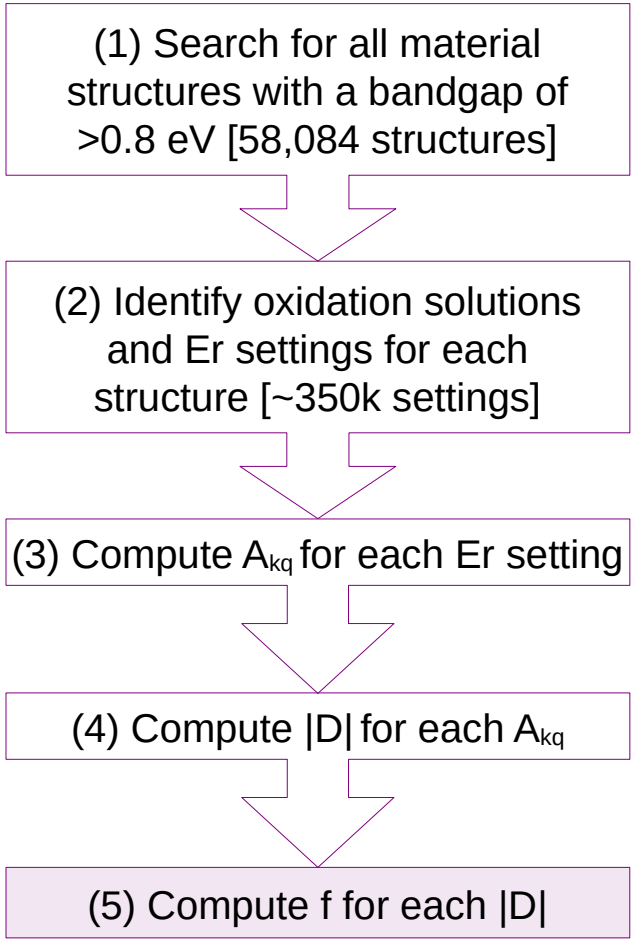


The Materials Project database allows for rapid processing of materials structures for identifying crystal hosts.

(1) In our initial search the only filter we apply is a bandgap of >0.8 eV, to facilitate our $Er^{3+}$ ~1.5μm transition.

*Later post-processing filtering may include, for example, selecting materials with constituent elements that must be enrichable to nuclear spin zero, to facilitate high spin coherence. [1]*

(2a) Multiple oxidation solutions result from ambiguous oxidation states. For example, $V_2NiO_6$ could have $V^{5+}$ and $Ni^{2+}$ or $V^{4+}$ and $Ni^{4+}$. We evaluate both of these cases.

(2b) Multiple settings arise from varying site symmetries and oxidation environments that $Er^{3+}$ can reside in. For example, $Y_2O_3$ has two inequivalent $Y^{3+}$ sites with $C_2$ and $C_{3i}$ symmetry.

[1]: Kanai et al., *PNAS*, 2022.

# Initial results from materials survey

THE UNIVERSITY OF CHICAGO
PRITZKER SCHOOL OF MOLECULAR ENGINEERING
Argonne NATIONAL LABORATORY
Q-NEXT NEXT GENERATION QUANTUM SCIENCE AND ENGINEERING

(1) Search for all material structures with a bandgap of >0.8 eV [58,084 structures]

(2) Identify oxidation solutions and Er settings for each structure [~350k settings]

(3) Compute $A_{kq}$ for each Er setting

(4) Compute |D| for each $A_{kq}$

(5) Compute f for each |D|

| Material | Er Site Info | $f_{el,calc}$ | $f_{el,lit}$ [1] |
|---|---|---|---|
| $LiNbO_3$ | Li site | 2e-6 | 1e-6 |
| $LiYF_4$ | Li site | 2e-7 | 2e-7 |
| $Y_2SiO_5$ | O-6 Y site | 2e-7 | 3e-7 |
| $Y_2SiO_5$ | PB-7 Y site | 9e-8 | 2e-8 |
| $CaWO_4$ | Ca site | 2e-7 | 2e-8 |

Preliminary agreement between calculations and literature. Tendency of the calculation to overestimate $f_{el}$.

*Recall that no fit parameters are involved here.*

*Note that f ~ 1e-6 yields a $T_1$ around 1 millisecond.*

[1] Thiel, Böttger, and Cone, *J. Lum.*, 131 253-361 (2011).

# Initial trends from materials survey



(1) Search for all material structures with a bandgap of >0.8 eV [58,084 structures]

(2) Identify oxidation solutions and Er settings for each structure [~350k settings]

(3) Compute $A_{kq}$ for each Er setting

(4) Compute |D| for each $A_{kq}$

(5) Compute f for each |D|

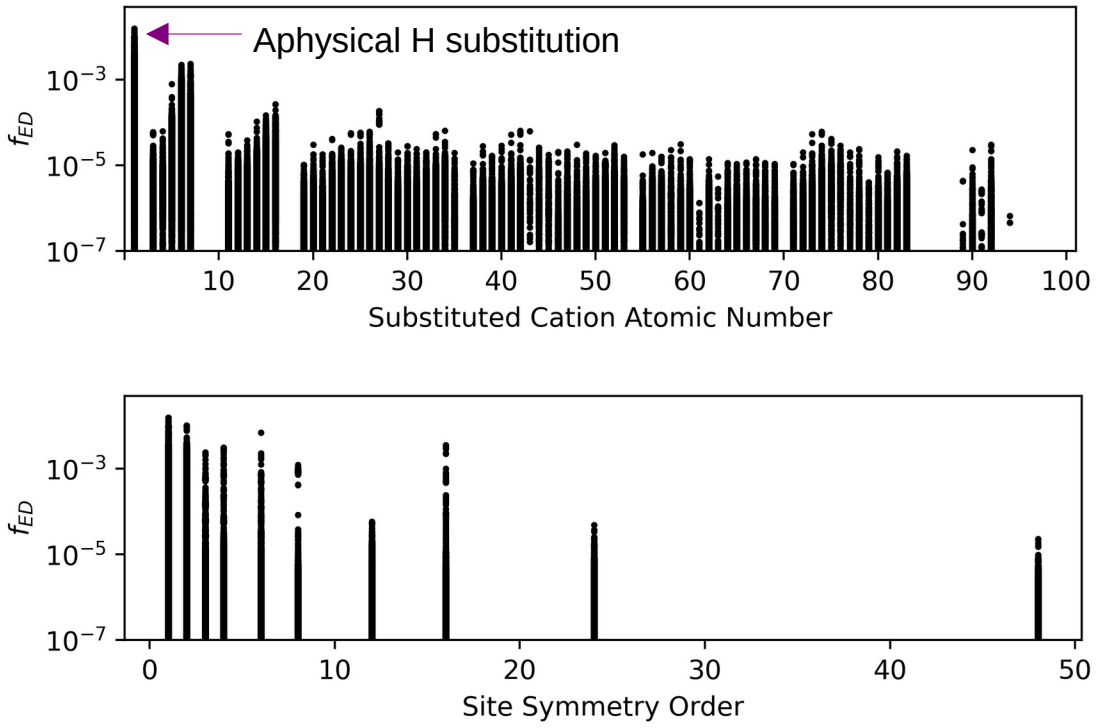


Each dot is one possible Er setting.
Higher *f* means brighter Er.

# Initial trends from materials survey



(1) Search for all material structures with a bandgap of >0.8 eV [58,084 structures]

(2) Identify oxidation solutions and Er settings for each structure [~350k settings]

(3) Compute $A_{kq}$ for each Er setting

(4) Compute |D| for each $A_{kq}$

(5) Compute f for each |D|

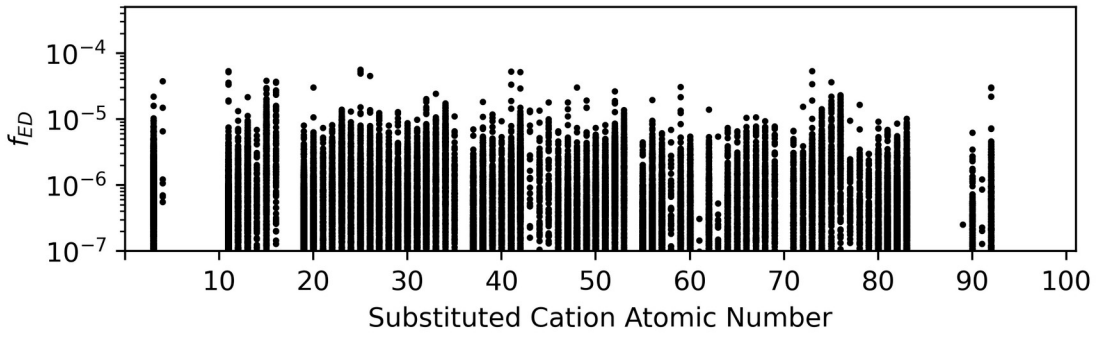


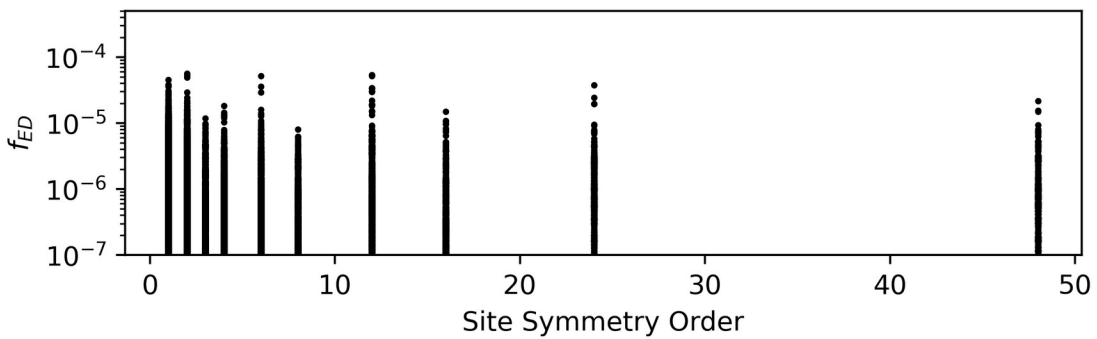


Each dot is one possible Er setting.
Higher *f* means brighter Er.

# Learning rules of thumb from survey

THE UNIVERSITY OF CHICAGO
PRITZKER SCHOOL OF MOLECULAR ENGINEERING
Argonne NATIONAL LABORATORY
Q-NEXT NEXT GENERATION QUANTUM SCIENCE AND ENGINEERING

(1) Search for all material structures with a bandgap of >0.8 eV [58,084 structures]

(2) Identify oxidation solutions and Er settings for each structure [~350k settings]

(3) Compute $A_{kq}$ for each Er setting

(4) Compute |D| for each $A_{kq}$

(5) Compute f for each |D|

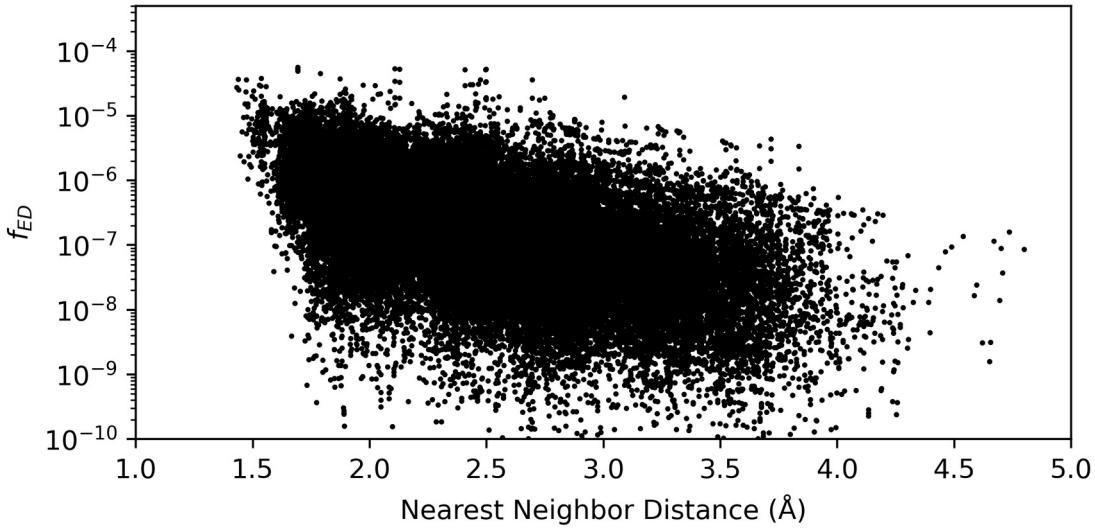


Correlation (Pearson r=-0.3) between nearest neighbor distance and oscillator strength (recall higher = brighter).

Parameters that do not show clear trends in brightness (here, |r|<0.1):
Site symmetry order, substituted atomic number,
material formation energy, material mass density

# Material candidates from survey



(1) Search for all material structures with a bandgap of >0.8 eV [58,084 structures]

(2) Identify oxidation solutions and Er settings for each structure [~350k settings]

(3) Compute $A_{kq}$ for each Er setting

(4) Compute |D| for each $A_{kq}$

(5) Compute f for each |D|

| Material | Er Site Info | $f_{el,calc}$ |
|---|---|---|
| $NaTaN_2$ | Na or Ta site | 5.3e-5 |
| $MoS_2$ | Mo site | 5.2e-5 |
| $Be_2C$ | Be site | 3.8e-5 |
| AlN | Al site | 2.2e-5 |
| $CeO_2$ | Ce site | 6.9e-6 |
| $Y_2O_3$ | $C_2$ Y site | 1.1e-6 |
| Rutile $TiO_2$ | Ti site | 7.2e-7 |
| Anatase $TiO_2$ | Ti site | 2.1e-7 |
| $Y_2O_3$ | $C_{3i}$ Y site | 1.6e-7 |

# Current status and next steps

THE UNIVERSITY OF CHICAGO
PRITZKER SCHOOL OF MOLECULAR ENGINEERING
Argonne NATIONAL LABORATORY
Q-NEXT NEXT GENERATION QUANTUM SCIENCE AND ENGINEERING

(1) Search for all material structures with a bandgap of >0.8 eV [58,084 structures]

(2) Identify oxidation solutions and Er settings for each structure [~350k settings]

(3) Compute $A_{kq}$ for each Er setting

(4) Compute |D| for each $A_{kq}$

(5) Compute f for each |D|

| Material | Er Site Info | $f_{el,calc}$ |
|---|---|---|
| $NaTaN_2$ | Na or Ta site | 5.3e-5 |
| $MoS_2$ | Mo site | 5.2e-5 |
| $Be_2C$ | Be site | 3.8e-5 |
| AlN | Al site | 2.2e-5 |

1) Account for refractive index in calculations, likely using dielectric constant $\varepsilon^{\infty}$ where available in Materials Project
2) Compute for specific transitions, e.g., $Y_1$ to $Z_1$
3) Identify methods to account for Er-substitution-induced strain

**4) Obtain bulk samples of promising materials for experimental doped Er brightness characterization**

5) Combine with nanophotonics for high-bandwidth Er defect engineering, up to the 100 kHz – 1 MHz range

# Thesis Defense Outline



1. Discussion on selecting a quantum communication-relevant defect
2. Review of erbium energy structure and aspects relevant to our work
3. Developing $CeO_2$ as a host for Er
4. Expanding $CeO_2$ to other substrates for alternative integrations
5. Considering other host materials for Er via computational survey
6. **Conclusions and final remarks**

# Conclusions and Final Remarks

THE UNIVERSITY OF CHICAGO
PRITZKER SCHOOL OF MOLECULAR ENGINEERING
Argonne NATIONAL LABORATORY
Q-NEXT NEXT GENERATION QUANTUM SCIENCE AND ENGINEERING

Er:$CeO_2$ is a promising quantum memory platform at 3.5 K, particularly at low doping levels of 2-3 ppm Er.

Oxygen anneals provide modest improvements.

**Spin echo and photon echo yield coherence times:**

**$T_{2,spin}$ = 0.25 ± 0.04 μs**

**$T_{2,optical}$ = 0.72 ± 0.03 μs**

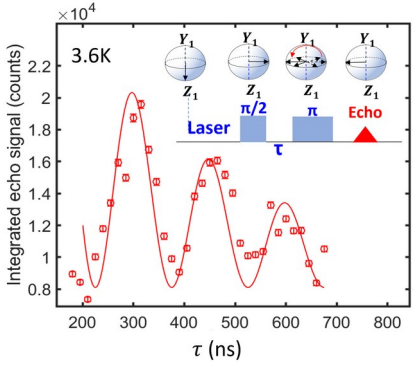



We may grow $CeO_2$(110) on Si(100), and its optical properties are no worse than on STO(001) except for shorter $T_1$.

This may make way for **new routes to Er:$CeO_2$ devices**, namely on SOI.

Via high-throughput computational survey, we have found additional viable hosts for Er that target **higher optical bandwidth**.

| Material | $f_{el,calc}$ |
|---|---|
| $NaTaN_2$ | 5.3e-5 |
| $MoS_2$ | 5.2e-5 |
| $Be_2C$ | 3.8e-5 |
| AlN | 2.2e-5 |

# Thank you for attending my thesis defense!

Thank you to everyone at the Guha Lab, Quantum Materials Lab, Freeland Lab, and others at Argonne!


Prof. Guha


Prof. Awschalom


Dr. Heremans


Dr. Dibos


Dr. Zhang


Dr. Sautter-Montoya


Dr. Chattaraj


Mr. Masiulionis

THE UNIVERSITY OF CHICAGO
PRITZKER SCHOOL OF MOLECULAR ENGINEERING

Argonne NATIONAL LABORATORY

Q-NEXT
NEXT GENERATION QUANTUM SCIENCE AND ENGINEERING

And thank you to all of my family and friends for your support during this marathon!

# Appendix Slides

# EPR Linewidth Supplemental

THE UNIVERSITY OF CHICAGO
PRITZKER SCHOOL OF MOLECULAR ENGINEERING
Argonne NATIONAL LABORATORY
Q-NEXT NEXT GENERATION QUANTUM SCIENCE AND ENGINEERING

Hamiltonian for two spins with dipolar interaction

$$H = \frac{g_1\mu_B}{2}\boldsymbol{\sigma}_1\cdot\boldsymbol{B} + \frac{g_2\mu_B}{2}\boldsymbol{\sigma}_2\cdot\boldsymbol{B} - \frac{\mu_0 g_1 g_2 \mu_B^2}{8\pi|\boldsymbol{r}|^3}\left(3(\boldsymbol{\sigma}_1\cdot\hat{\boldsymbol{r}})(\boldsymbol{\sigma}_2\cdot\hat{\boldsymbol{r}}) - \boldsymbol{\sigma}_1\cdot\boldsymbol{\sigma}_2\right)$$

Energy shift on spin 1 due to dipolar interaction with spin 2

$$\epsilon(\boldsymbol{r},\pm) = \pm 2\gamma = \pm\frac{\mu_0 g_1 g_2 \mu_B^2}{4\pi|\boldsymbol{r}|^3}(3\cos^2\theta - 1)$$

Linewidth (Lorentzian, in Hz) due to an ensemble of interacting spins with g-factor *g* and concentration *C* (#/m³)

$$\Gamma_{\mathrm{EPR}} > \Gamma_{dd} = \frac{\pi}{9\sqrt{3}}\frac{\mu_0(g\mu_B)^2}{h}C$$

$\mu_0$ = 1.256637e-6 T²m³/J
$\mu_B$ = 9.27401e-24 J/T
h = 6.62607e-34 J/Hz

Sanity check: g=2 and C=$10^{18}$ $cm^{-3}$ should yield ~132 kHz
Indeed, yields 131.5 kHz! (exercise from Geschwind)

For 10 ppm in $CeO_2$: g=6.812, C=7.6x$10^{17}$ $cm^{-3}$
**10 ppm yields $\Gamma_{d\text{-}d}$ = 1.15 MHz, 100 ppm yields 15.2 MHz**

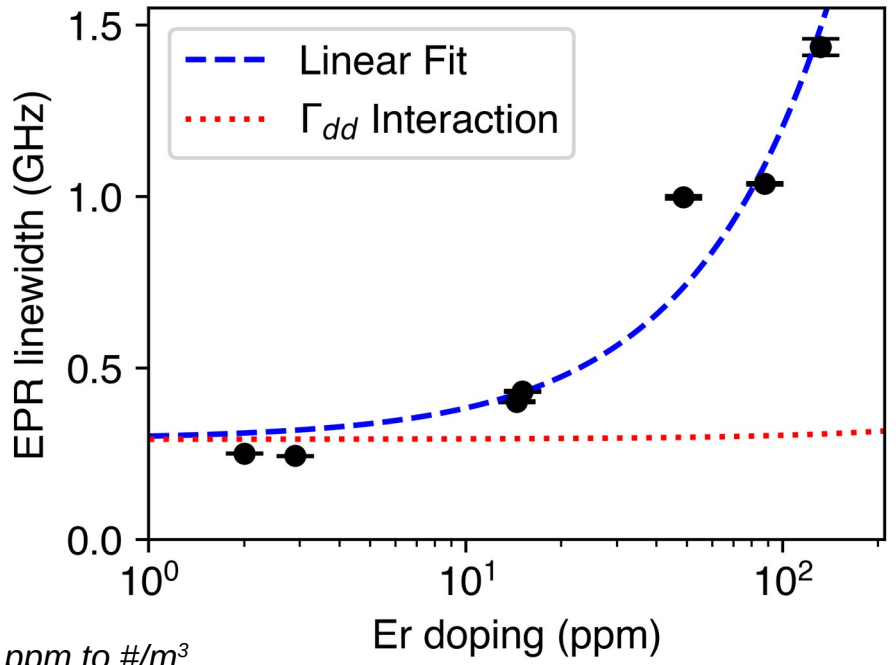


*ppm to #/m³*

decimal = ppm/1e6
$CeO_2$ atoms/m³ = 12 / (5.411e-10 m)³ = 7.57e28 atoms/m³
ppm = decimal * 7.57e28 Er/m³ (or: decimal * 7.57e22 Er/cm³)

Ex: 10 ppm = (10/1e6) * 7.57e28 $m^{-3}$ = 7.57e17 $cm^{-3}$

# Cubic locations in the $CeO_2$ lattice

THE UNIVERSITY OF CHICAGO
PRITZKER SCHOOL OF MOLECULAR ENGINEERING
Argonne NATIONAL LABORATORY
Q-NEXT NEXT GENERATION QUANTUM SCIENCE AND ENGINEERING

There are three intrinsic disorder processes in $CeO_2$, and three extrinsic disorder processes incorporating $M_2O_3$ that yield from those intrinsic processes. (Minervini et al, 1998, Solid State Ionics)

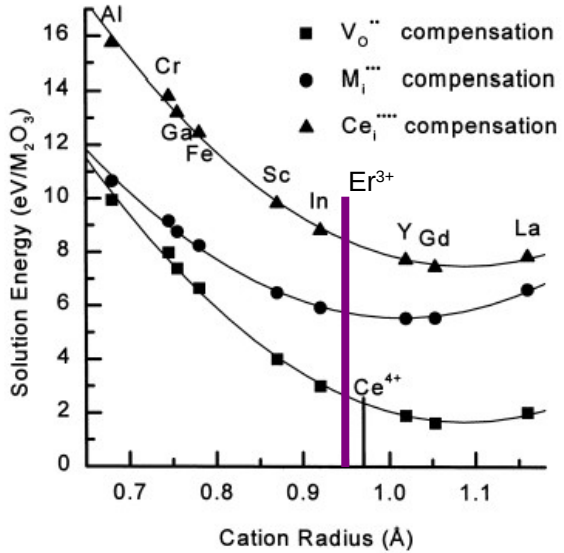


Fig. 1. Solution energies for the incorporation of $M_2O_3$ into $CeO_2$ assuming isolated point defects.

Vacancy compensation

$$M_2O_3 \leftrightarrow 2M'_{Ce} + V_O^{\bullet\bullet} + 3O_O^{\times}$$

Dopant interstitial compensation

$$2M_2O_3 \leftrightarrow 3M'_{Ce} + M_i^{\bullet\bullet\bullet} + 6O_O^{\times}$$

Cerium interstitial compensation

$$Ce_{Ce}^{\times} + 2O_O^{\times} + 2M_2O_3 \leftrightarrow 4M'_{Ce} + Ce_i^{\bullet\bullet\bullet\bullet} + 8O_O^{\times}$$

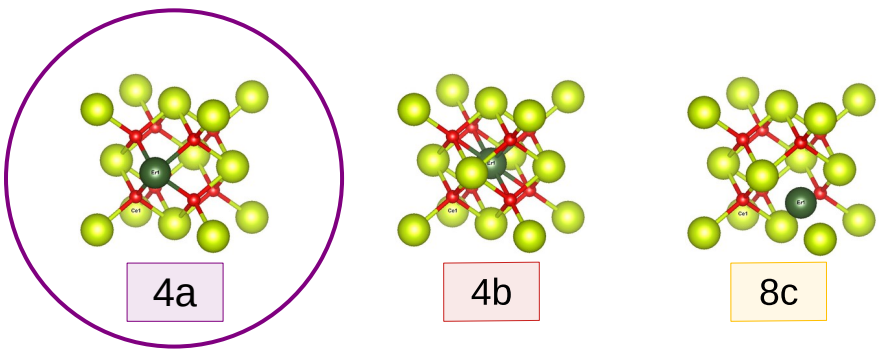


**If vacancy compensation dominates, then the trivalent dopant preferentially substitutes into the Ce site** (4a) instead of the interstitial site (4b). Experimental work in low-doped $Fe^{3+}$:$CeO_2$ verifies this (Bao et al, 2008, Catal Lett).

# Stoneham's equations supplemental

THE UNIVERSITY OF CHICAGO
PRITZKER SCHOOL OF MOLECULAR ENGINEERING
Argonne NATIONAL LABORATORY
Q-NEXT NEXT GENERATION QUANTUM SCIENCE AND ENGINEERING

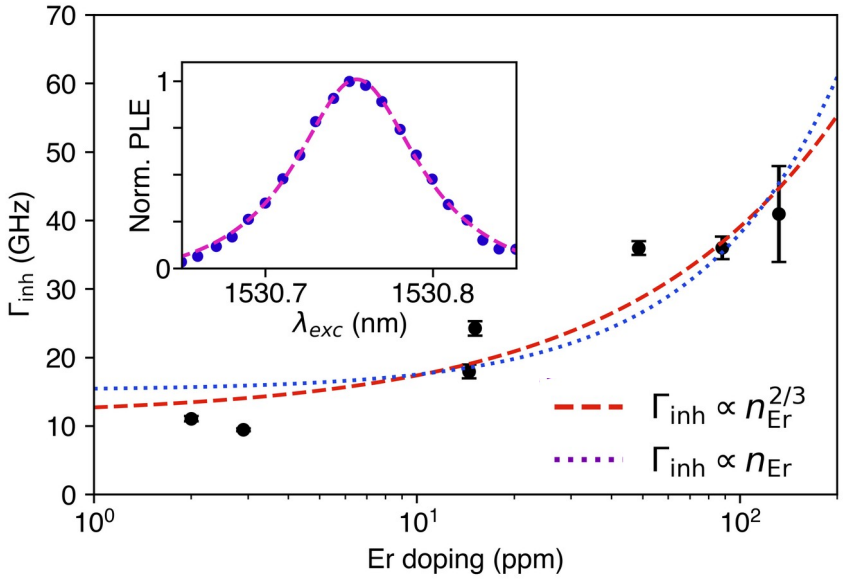


$$I(\omega) = \frac{1}{2\pi} \int_{-\infty}^{+\infty} d\rho \exp\{-ix\omega\}\left(1 - J/V\right)^N$$

$$J = \int^{V} \left(1 - \exp\{ix\epsilon(\boldsymbol{z})\}\right) p(\boldsymbol{z}) d\boldsymbol{z}$$

REVIEWS OF MODERN PHYSICS VOLUME 41, NUMBER 1 JANUARY 1969

## Shapes of Inhomogeneously Broadened Resonance Lines in Solids

A. M. STONEHAM
*Theoretical Physics Division, Atomic Energy Research Establishment, Harwell, Berkshire, England*

Inhomogeneous broadening has been observed in resonance lines in solids over the wide range of energies spanned by nuclear magnetic resonance, electron spin resonance, optical, and Mössbauer methods. The broadening arises from random strains, electric fields, and other perturbations from the defects in the lattice containing the centre whose transitions are studied. This paper reviews the calculation of the shapes of such resonance lines. The most important method

# Inokuti-Hirayama supplemental



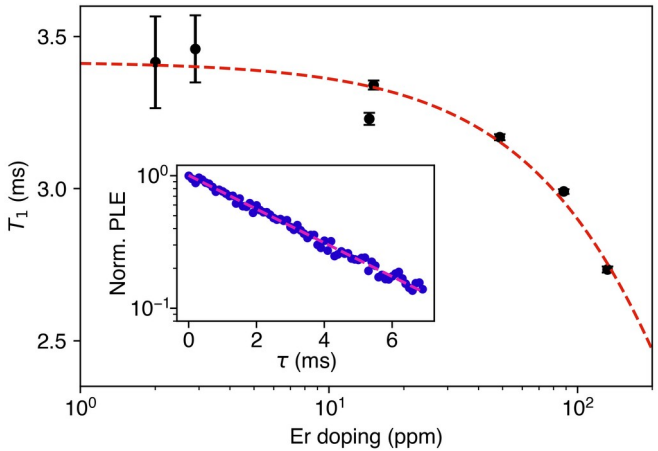


$$\phi(t) = \phi_0 \exp\left[-\frac{t}{T_1^{(0)}} - \Gamma\left(1-\frac{3}{\nu}\right)\frac{n}{n_0}\left(\frac{t}{T_1^{(0)}}\right)^{3/\nu}\right]$$

$$T_1 = \int_0^\infty t\phi(t)dt \Big/ \int_0^\infty \phi(t)dt$$

THE JOURNAL OF CHEMICAL PHYSICS VOLUME 43, NUMBER 6 15 SEPTEMBER 1965

## Influence of Energy Transfer by the Exchange Mechanism on Donor Luminescence*

MITIO INOKUTI AND FUMIO HIRAYAMA†
*Argonne National Laboratory, Argonne, Illinois*
(Received 17 May 1965)

The decay of donor luminescence in a rigid solution when modified by electronic energy transfer by the exchange mechanism is treated theoretically. The rate constant for the elementary process of energy transfer

# Optical echo vs temperature details

THE UNIVERSITY OF CHICAGO
PRITZKER SCHOOL OF MOLECULAR ENGINEERING
Argonne NATIONAL LABORATORY
Q-NEXT NEXT GENERATION QUANTUM SCIENCE AND ENGINEERING

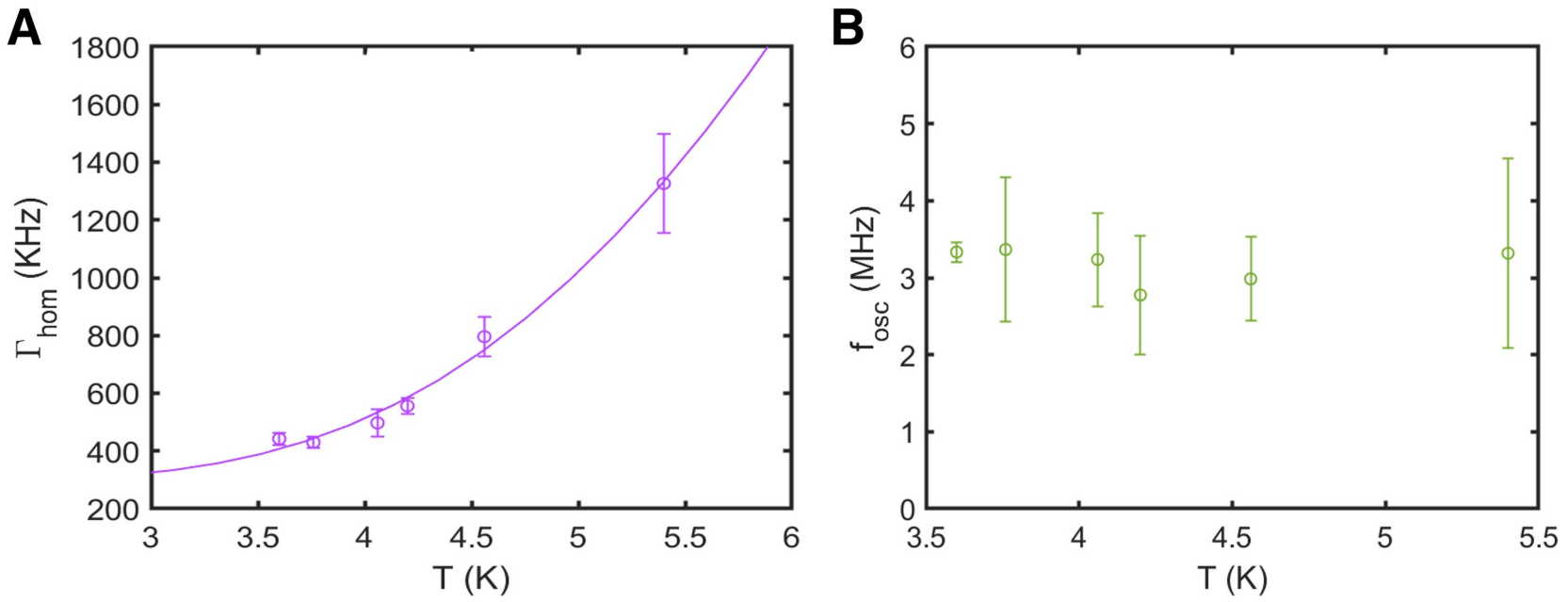


We see broadening of the optical homogeneous linewidth as a function of temperature, but the coherent beating does not change frequency.

$$\Gamma_{\mathrm{hom}}(T) = \Gamma_0 + \alpha_{\mathrm{TLS}} T + \alpha_{\mathrm{phonon}} \exp\{-\Delta E / k_B T\}$$



Zhang et al, arXiv:2309.16785 (2023)

# Optical spin $T_1$ measurements



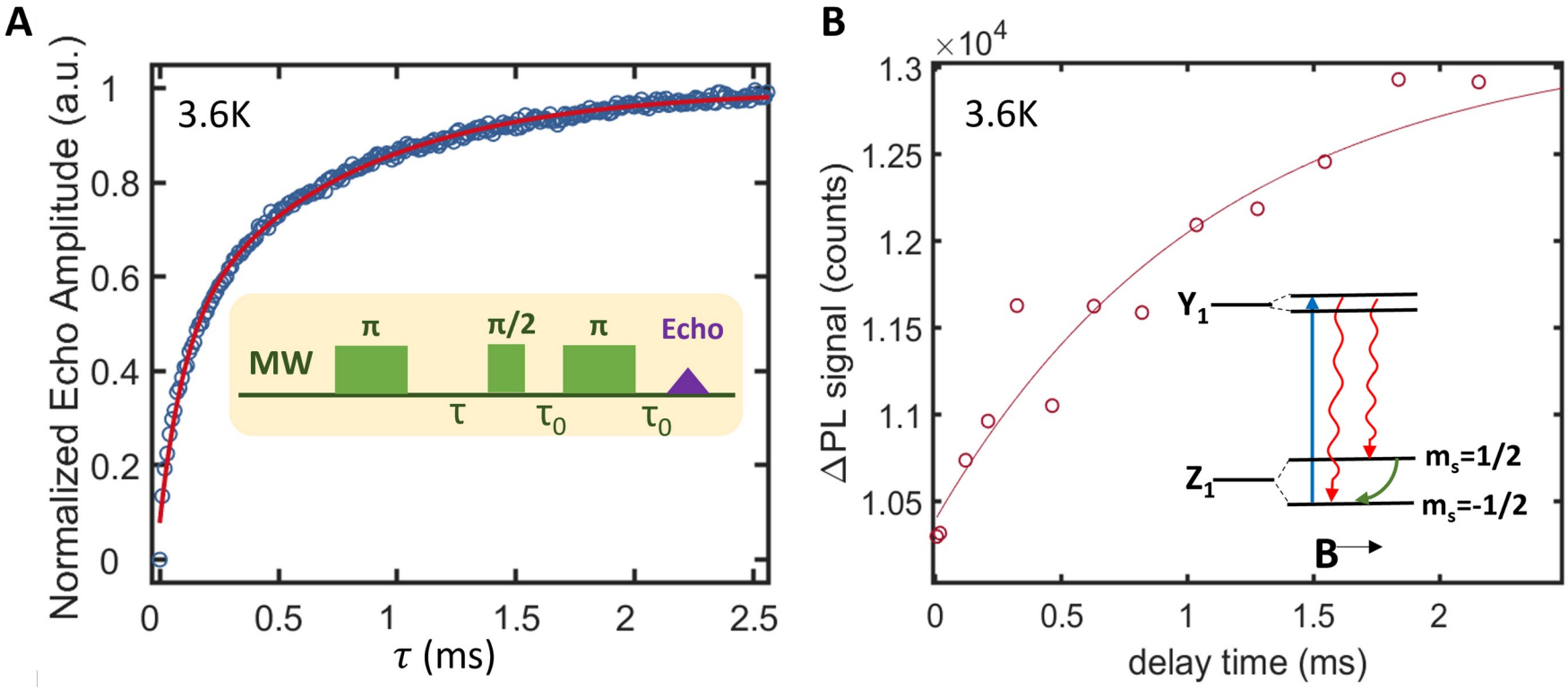




Zhang et al, arXiv:2309.16785 (2023)

# Electric dipole matrix elements



The matrix element of the dipole operator ($D_\rho^{(1)} \sim r$) is evaluated in the crystal field-perturbed basis B, when transitioning from state B to state B', as shown here in (1). Judd (1962) [1] lays this out.

$$(1): \quad \langle B| D_\rho^{(1)} |B'\rangle = \sum_{k,q,\ \text{even}\ \lambda} (2\lambda+1)(-1)^{q+\rho} A_q^{(k)} \begin{pmatrix} 1 & \lambda & k \\ \rho & -q-\rho & q \end{pmatrix} \langle A| U_{q+\rho}^{(\lambda)} |A'\rangle \, \Xi(k,\lambda)$$

We then need to compute the connection between the unperturbed states A and A', using definitions available in Wybourne (1965). The reduced matrix elements at the end may be looked up in, e.g., Nielson & Koster (1963).

$$(2): \quad \langle A| U_{q+\rho}^{(\lambda)} |A'\rangle = \sum_{M,M'} a_M a_{M'} \left\langle l^N \gamma S L J M \middle| U_{q+\rho}^{(\lambda)} \middle| l^N \gamma' S' L' J' M' \right\rangle$$

$$\left\langle l^N \gamma S L J M \middle| U_{q+\rho}^{(\lambda)} \middle| l^N \gamma' S' L' J' M' \right\rangle = (-1)^{J-M+S+L+J'+\lambda} \sqrt{(2J+1)(2J'+1)} \times \begin{pmatrix} J & \lambda & J' \\ -M & q+\rho & M' \end{pmatrix} \begin{Bmatrix} J & J' & \lambda \\ L' & L & S \end{Bmatrix} \left\langle l^N \gamma S L \middle| \middle| U^{(\lambda)} \middle| \middle| l^N \gamma' S' L' \right\rangle$$

Finally, the evaluation of the term Ξ at the end of (1) is provided by Judd; he also includes radial wavefunction integral expressions and energies for $Er^{3+}$.

$$(3): \quad \Xi(k,\lambda) = 2 \sum_{n',l'} (2l+1)(2l'+1)(-1)^{l+l'} \begin{Bmatrix} 1 & \lambda & k \\ l & l' & l \end{Bmatrix} \begin{pmatrix} l & 1 & l' \\ 0 & 0 & 0 \end{pmatrix} \begin{pmatrix} l' & k & l \\ 0 & 0 & 0 \end{pmatrix} \frac{\langle nl| r |n'l'\rangle \langle nl| r^k |n'l'\rangle}{\Delta(n'l')}$$



[1]: Judd, *Physical Review*, 1962.